

Advanced Diagnostics for Electric Space Propulsion

Thomas Trottenberg

Florian Bansemer, Marcel Hesse, Holger Kersten, Mathis Klette, Jens Laube, Viktor Schneider, Björn Schuster, Lars Seimetz, Alexander Spethmann, Robert Wimmer-Schweingruber



GEC IOPS, March 27th, 2025

International Online Plasma Seminar (IOPS)

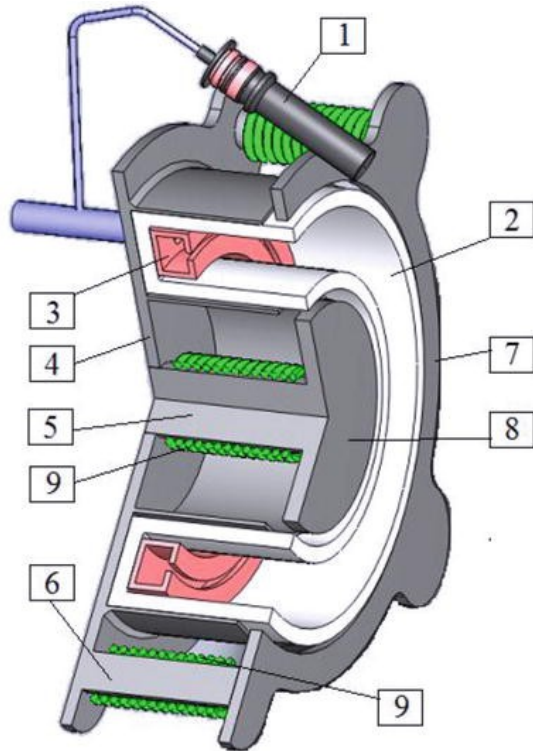
Outline

1. Standard Diagnostics in EP Development and Testing
2. Force probes as a novel Diagnostic
3. The EPDP for the Heinrich Hertz Satellite
4. Data from the Plasma Sensor
5. Unexpected Features of the Retarding Potential Analyzer
6. Conclusion

Standard Diagnostics in EP Development and Testing

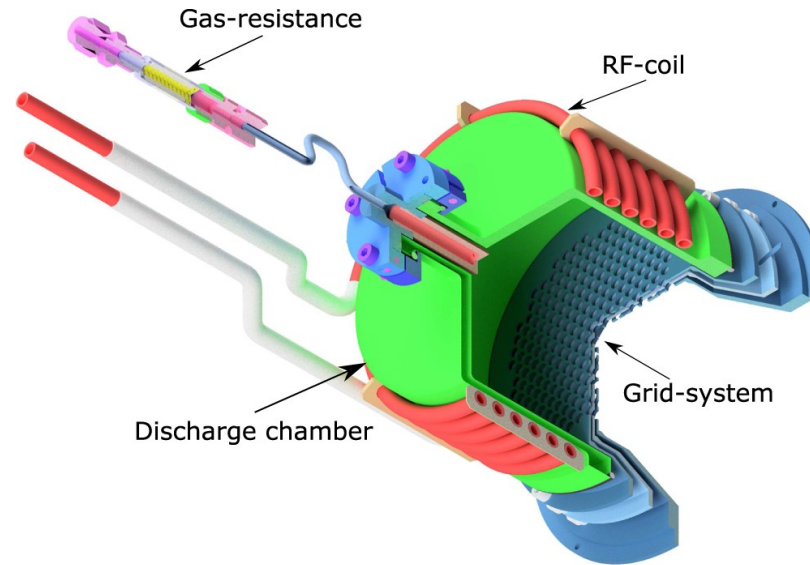
Some Important Thruster Types

Hall Thruster



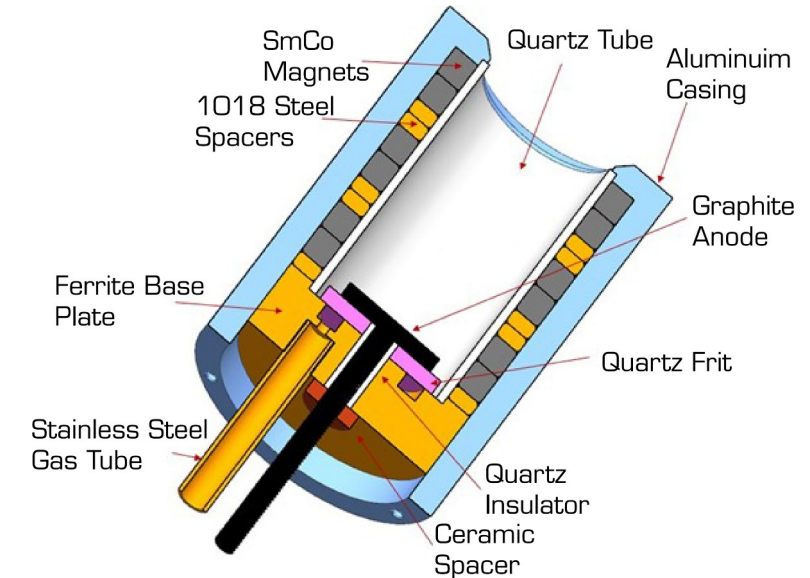
A. V. Loyan and A. N. Khaustova, Hall Thruster Erosion. IntechOpen (2019). <https://doi.org/10.5772/intechopen.82654>

Gridded Ion Thruster



P. Dietz et al., Plasma Sources Sci. Technol. 28, 084001 (2019)

High-Efficiency Multistage Plasma Thruster (HEMPT)



Saridede, Yediyildiz, and Celik, J. Aerosp. Technol. Manag. 15 (2023) <https://doi.org/10.1590/jatm.v15.1294>

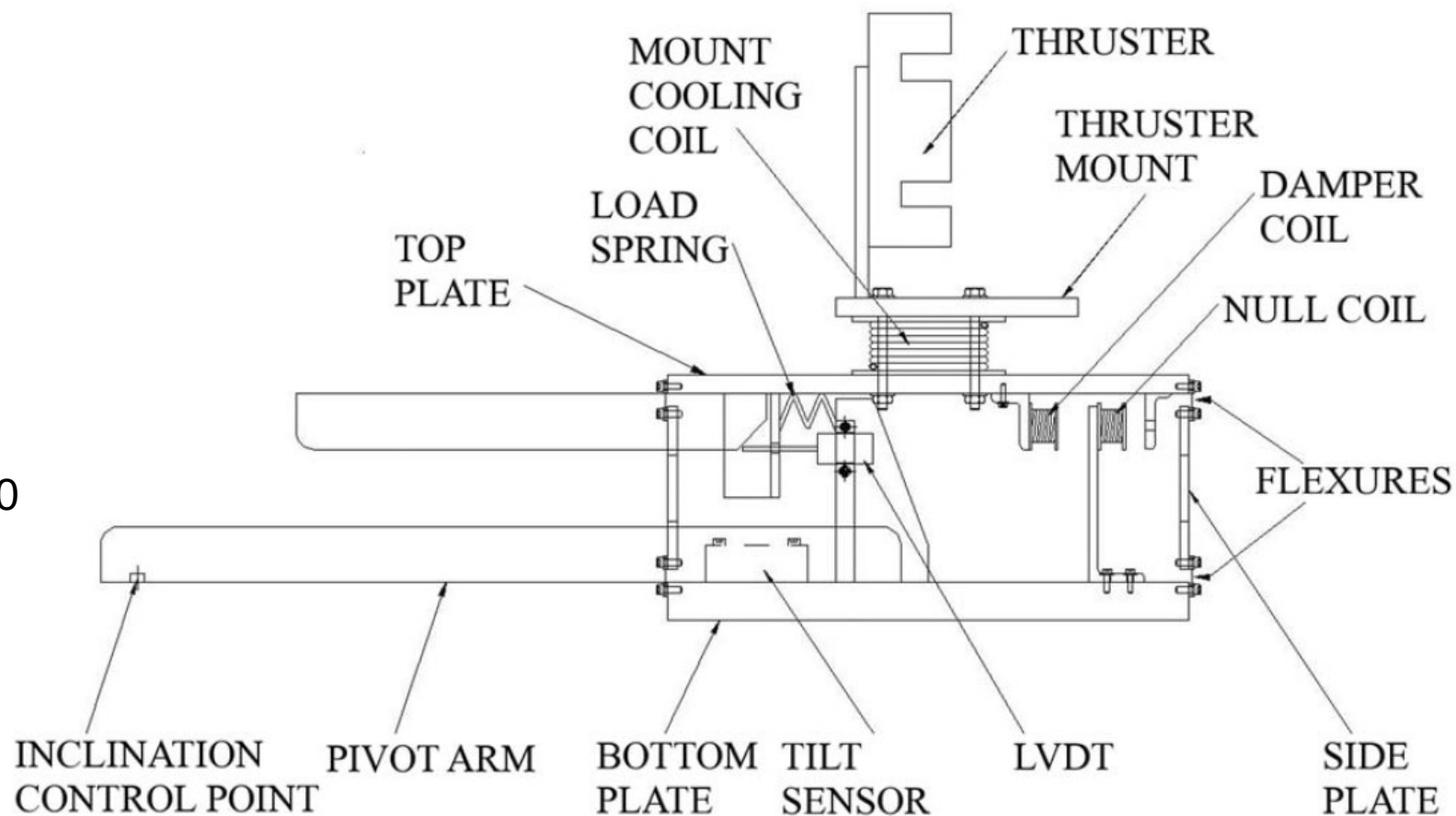
Direct Thrust Measurements

Example of a thrust balance:

Inverted Pendulum Thrust Balance

Challenges:

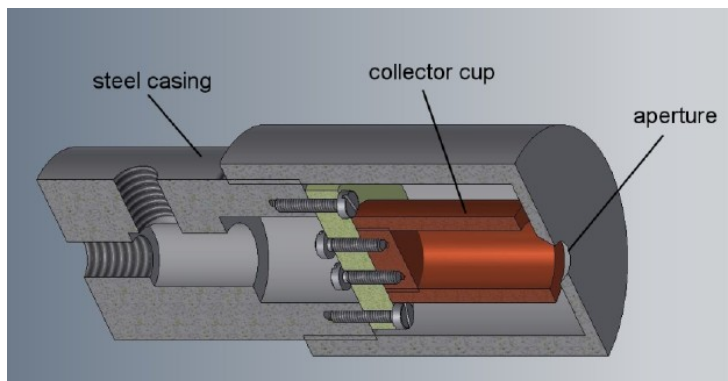
- Thrust-to-weight ratio often $< 1:500$
- Cables, gas feeds act like springs



Xu and Walker, Rev. Sci. Instrum. 80, 055103 (2009)

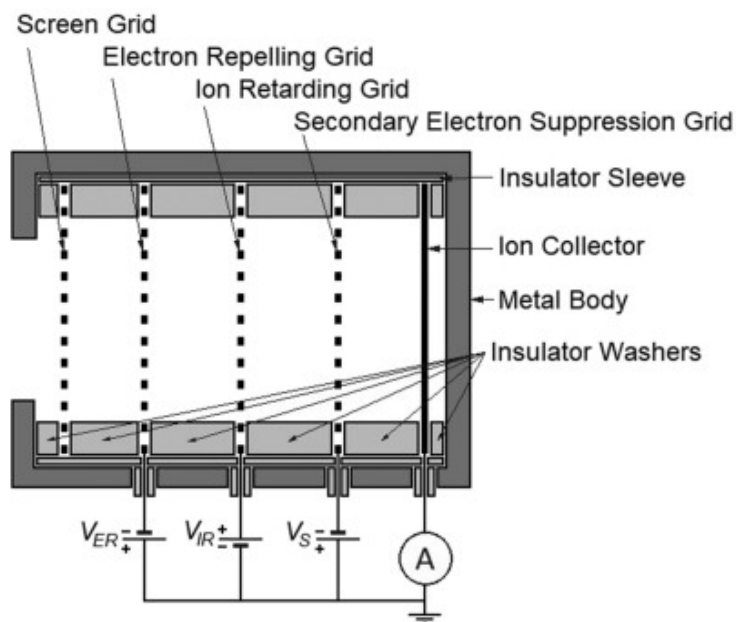
Standard Diagnostics mostly measure Currents

Faraday Cup



A. Spethmann et al., Rev. Sci. Instrum. 86,015107 (2015)

Retarding Potential Analyzer



Maystrenko et al., Rev. Sci. Instrum. 93,073504 (2022)

Others

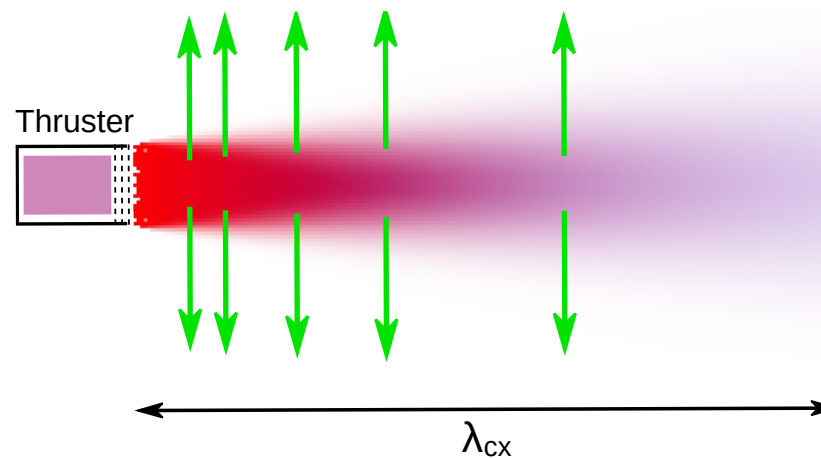
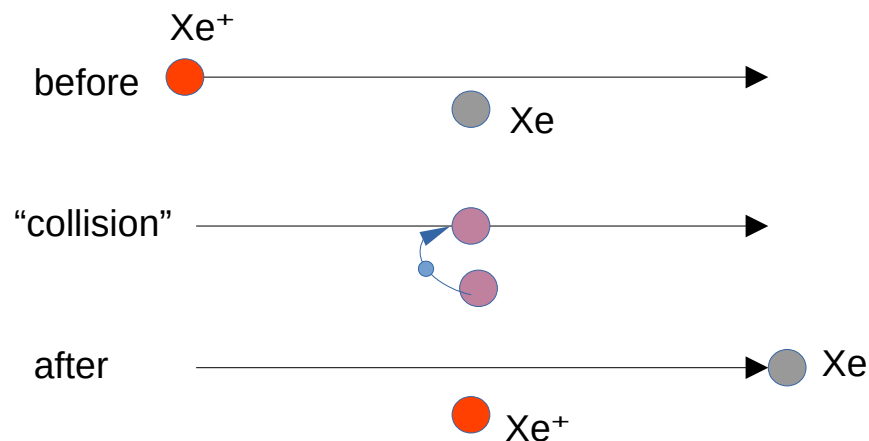
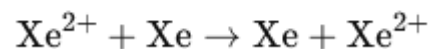
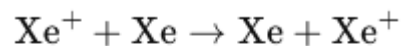
- Langmuir probes
- „Faraday probes“

Less common in test facilities,
more common in
research laboratories:

- Emission spectroscopy
- Laser induced fluorescence
- Quadrupole mass spectrometry
- ExB probe (Wien or velocity filter)
- Electrostatic filters

The Challenge of Charge-Exchange Collisions

CEX collision reactions:

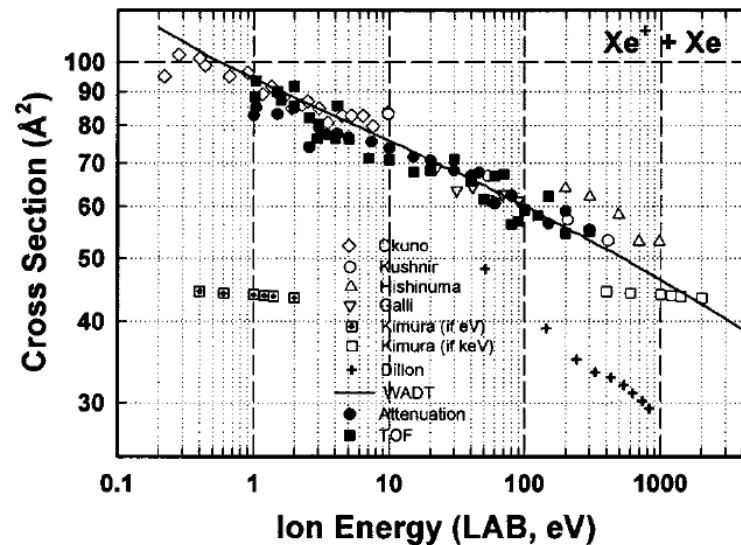


Example:

$$\rho = 10 \text{ mPa}$$

$$E_{\text{kin}} = 1200 \text{ eV}$$

$$\rightarrow \lambda_{\text{cx}} = 0.92 \text{ m}$$



Miller and Pullins, J. Appl. Phys. 91, 984 (2002)

Why are CEX collisions important?

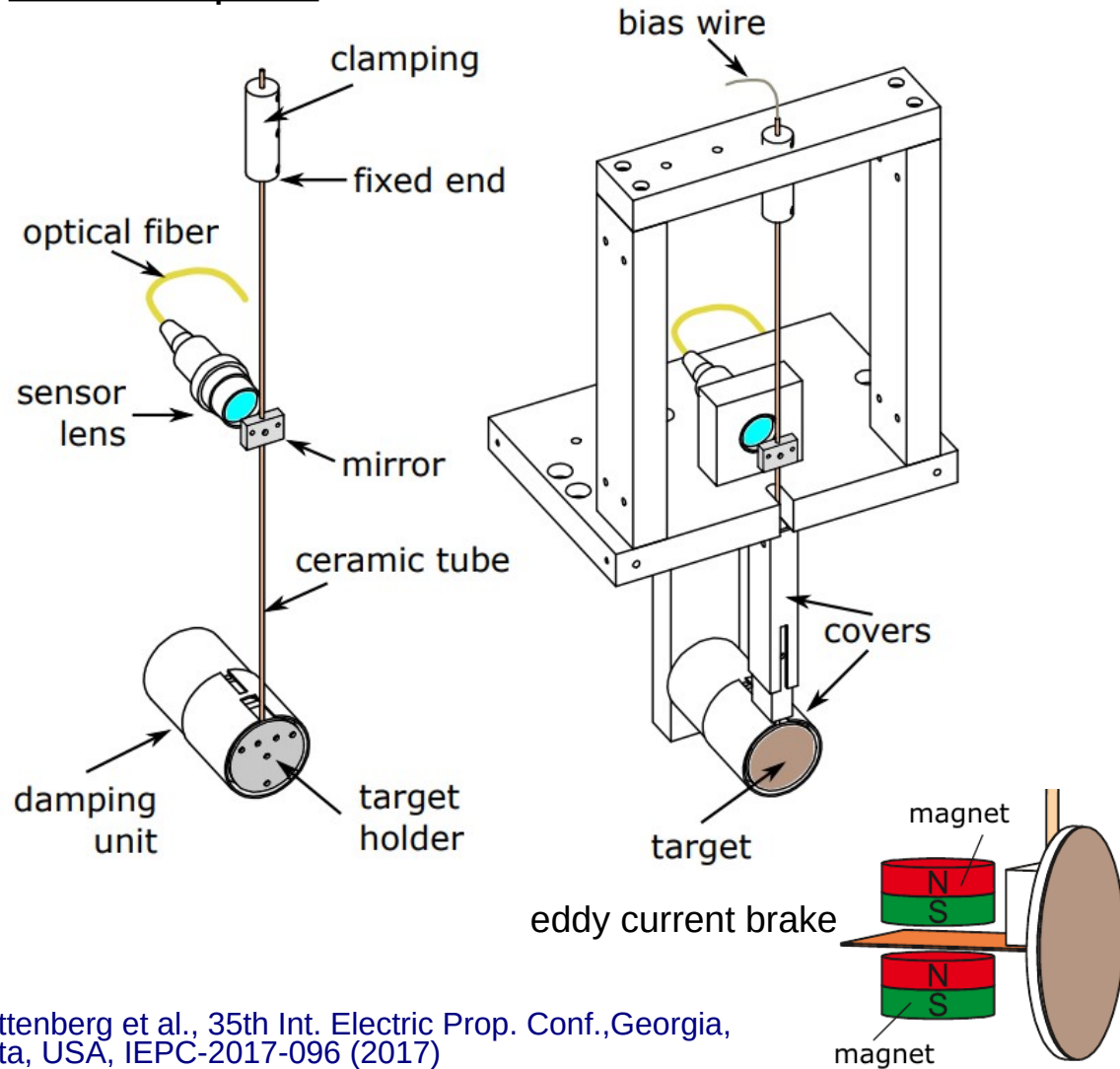
Electrostatic diagnostics can only measure currents

Thermal (slow) ions are released at elevated potentials and return to the spacecraft with high kinetic energies (sputtering)

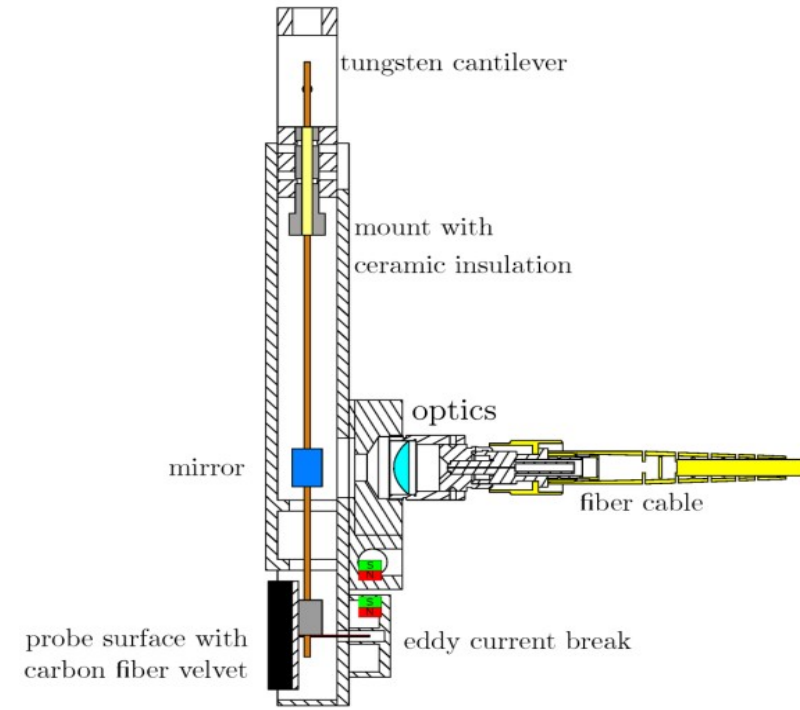
Force Probes as a Novel Diagnostic

Force Probes as a Novel Thruster Diagnostic

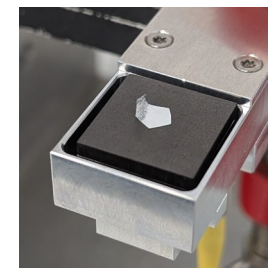
Essential parts



Compact version of the force probe



Klette et al., J. Vac. Sci. Technol. A 38, 033013 (2020)



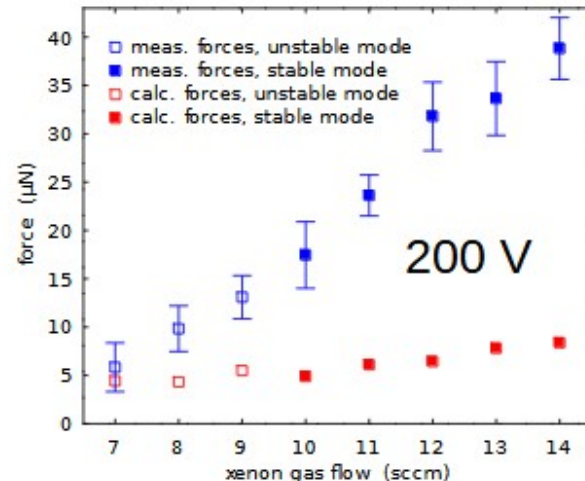
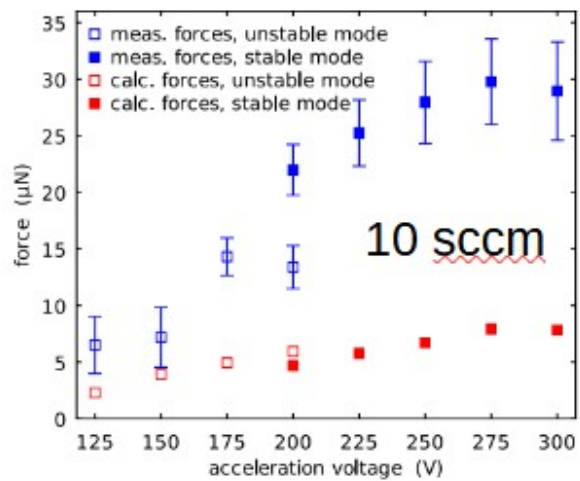
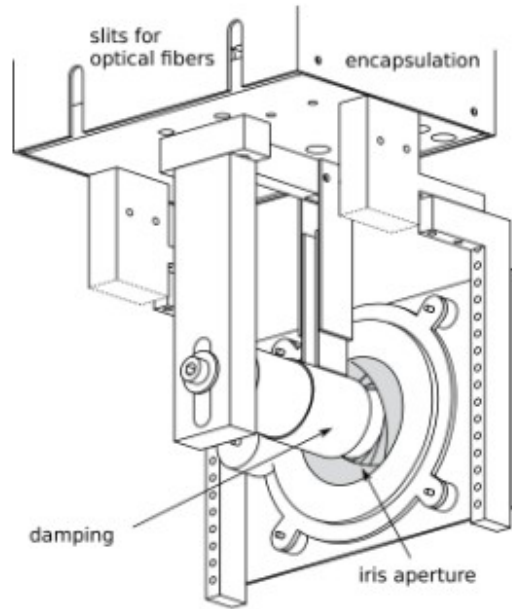
Calibration with mg weights

T. Trottenberg et al., 35th Int. Electric Prop. Conf., Georgia, Atlanta, USA, IEPC-2017-096 (2017)

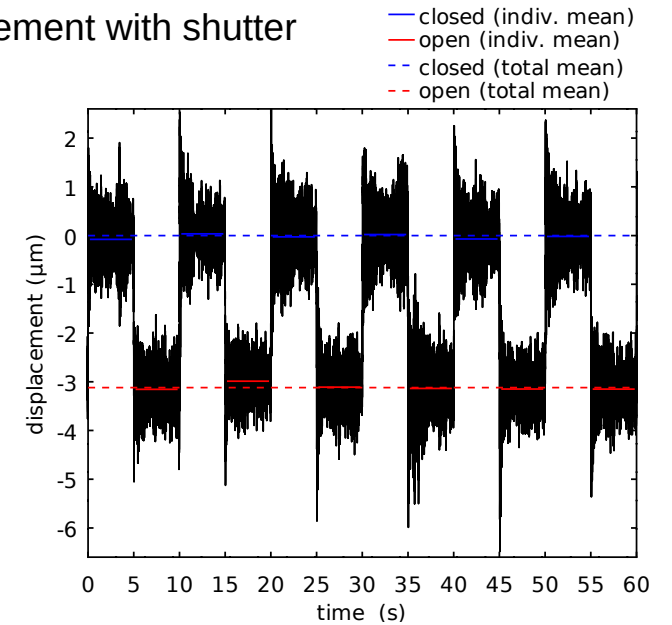
Force Probes as a Novel Thruster Diagnostic



ISCT200-MS Hall thruster



Measurement with shutter

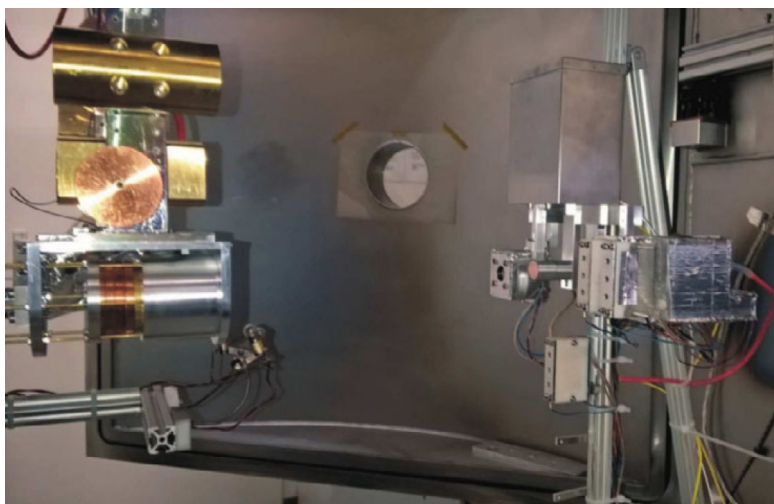


Measurement in der "NexET" chamber at ICARE in Orléans.

- Simultaneous current measurement with the grounded target
- Currents include electrons
- Calculation of the force from the measured electric currents underestimates the real forces

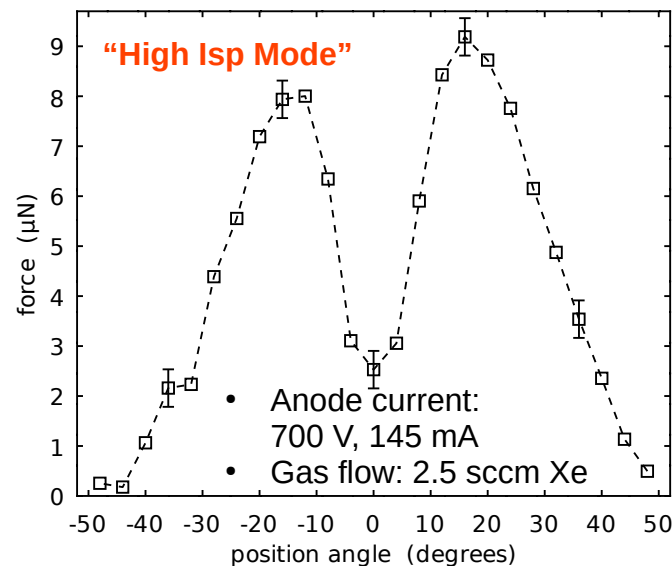
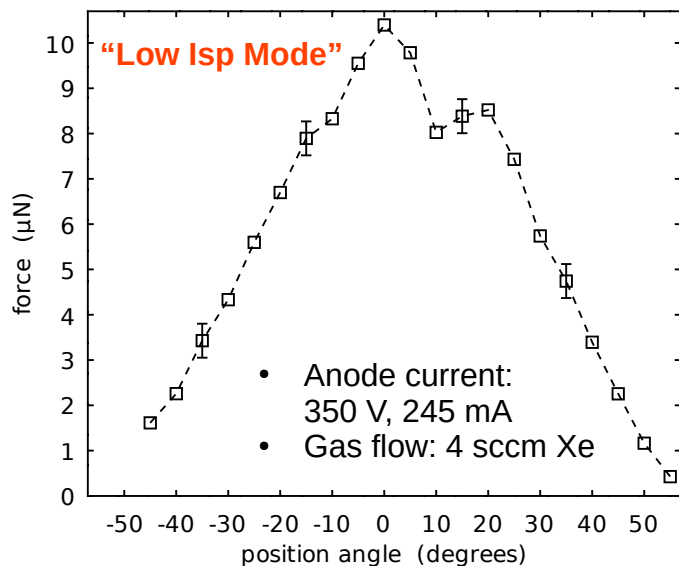
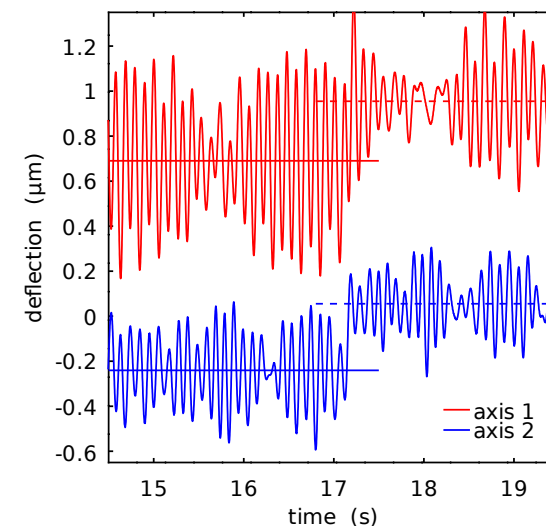
Spethmann et al., EPJ Techn.Instrum. 9, 4 (2022)

Force Probes as a Novel Thruster Diagnostic



Measurement at the *Laboratory for Enabling Technologies*, Airbus, Friedrichshafen, Germany.

- Swivel arm (constant distance)
- Integration of the momentum flux density agrees with direct thrust measurement (thrust balance)
- Forces calculated from currents underestimate the real forces (charge-exchange collisions)

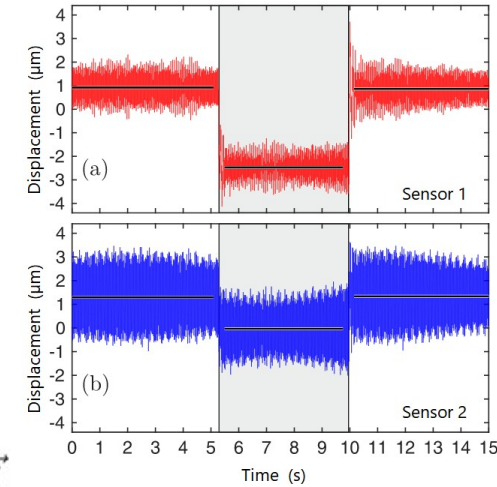
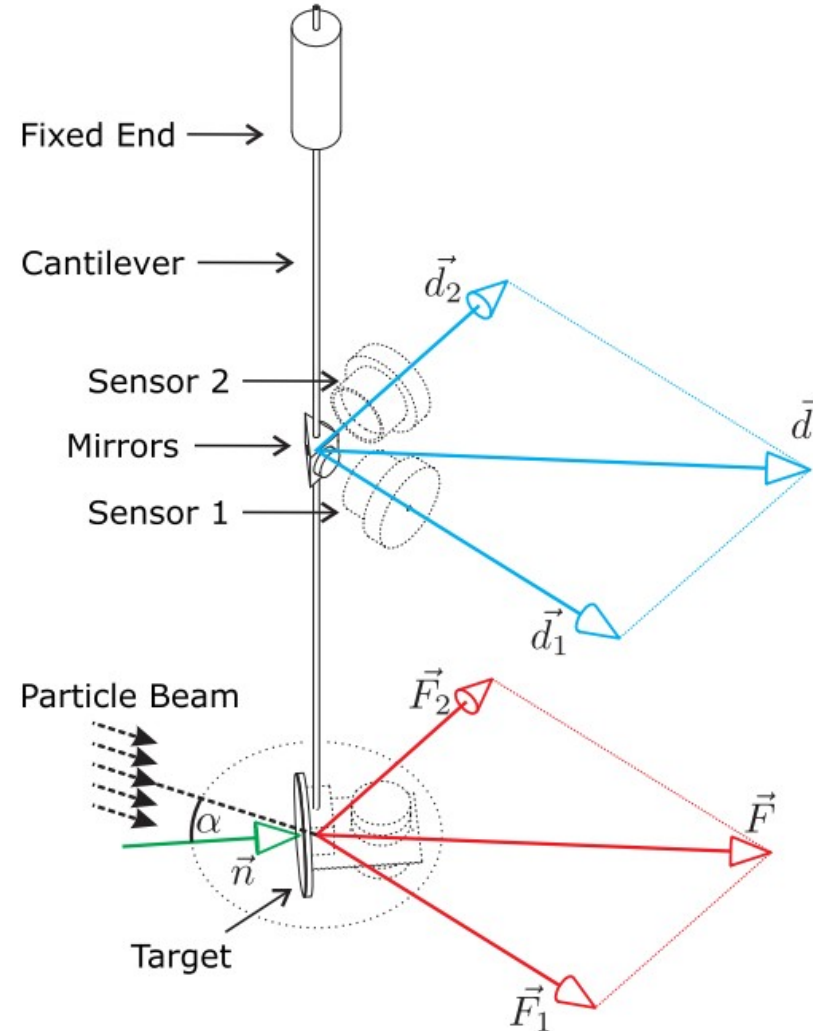
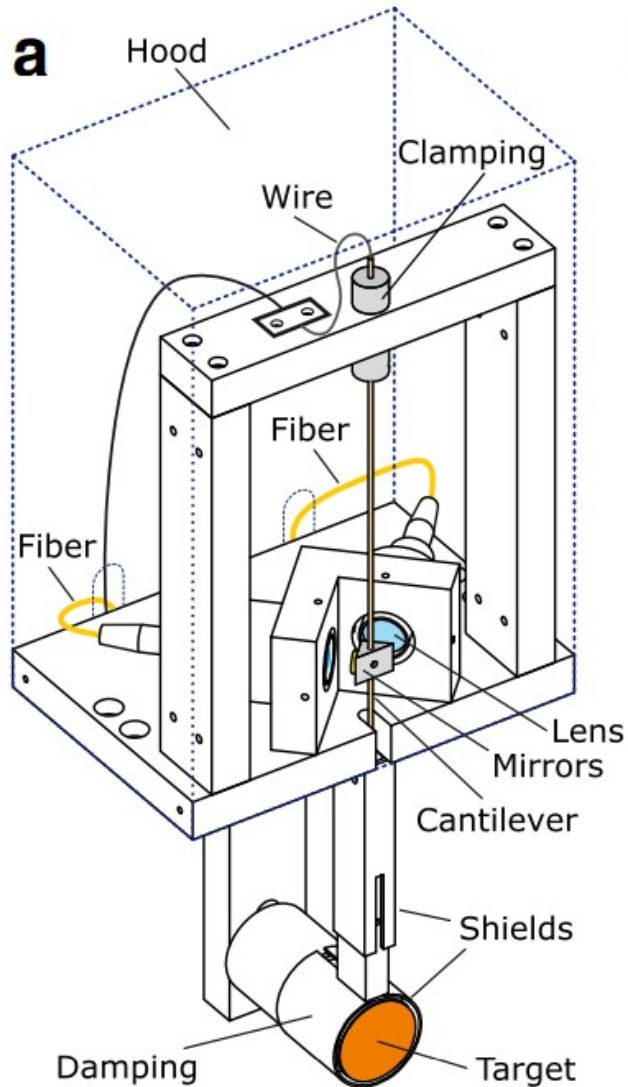


Comparison with thrust balance

- “High Isp Mode”:
Integration: 2.9 mN,
Balance: 3236 μN
- “Low Isp Mode”:
Integration: 3.6 mN,
Balance: 3200 μN

Spethmann et al., EPJ Techn.Instrum. 9, 4 (2022)

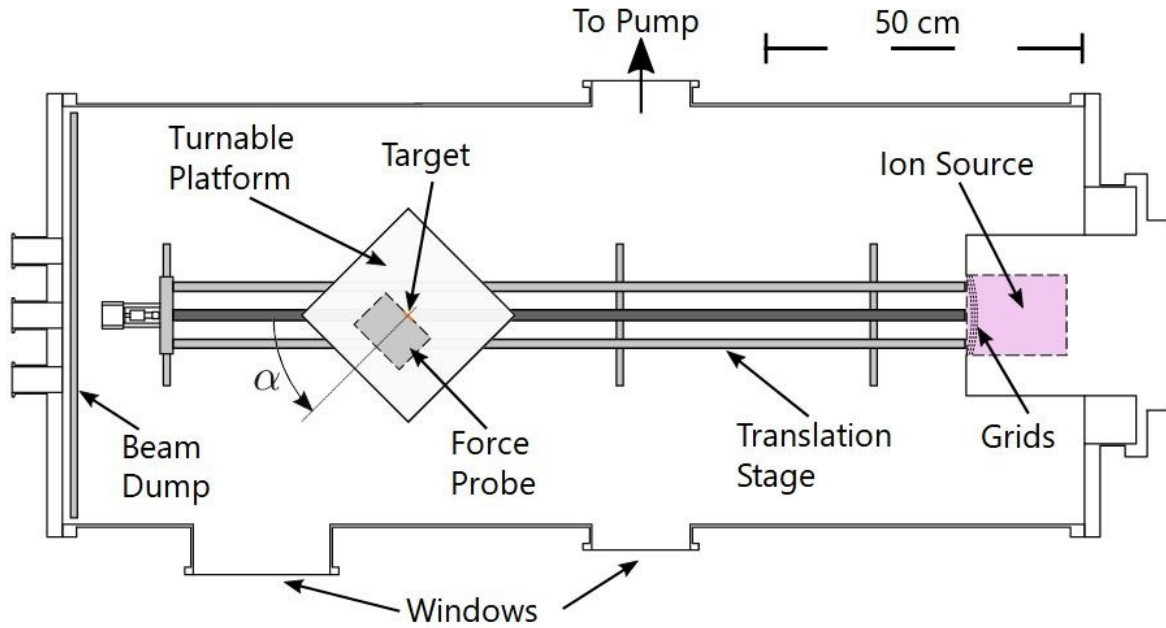
Force Probes for the Study of Sputtering



The two-axis probe measures force as a 2d vector

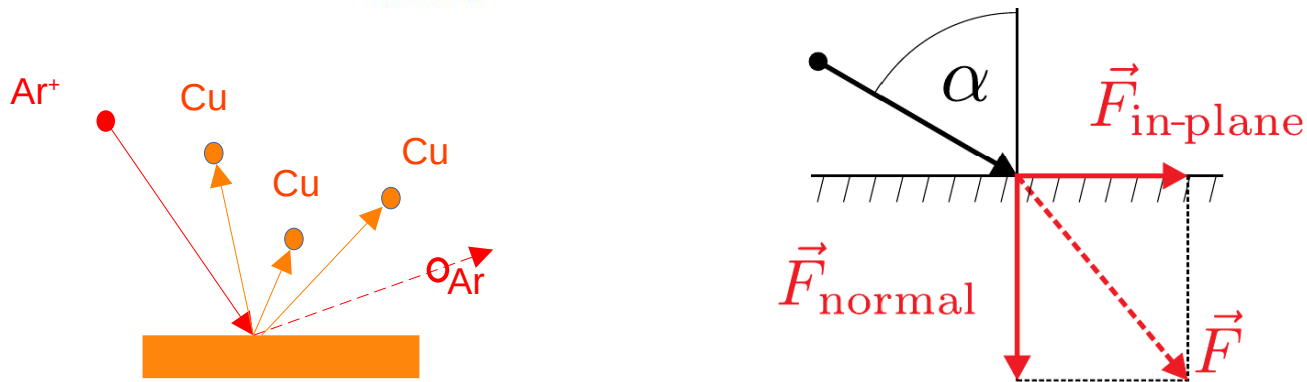
Trottenberg et al., EPJ Techn. Instrum. 5, 3 (2018)

Force Probes for the Study of Sputtering

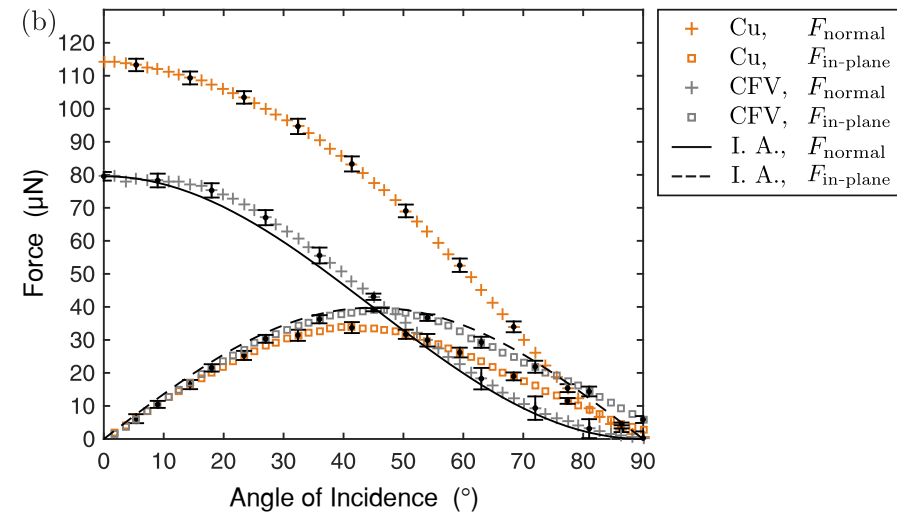
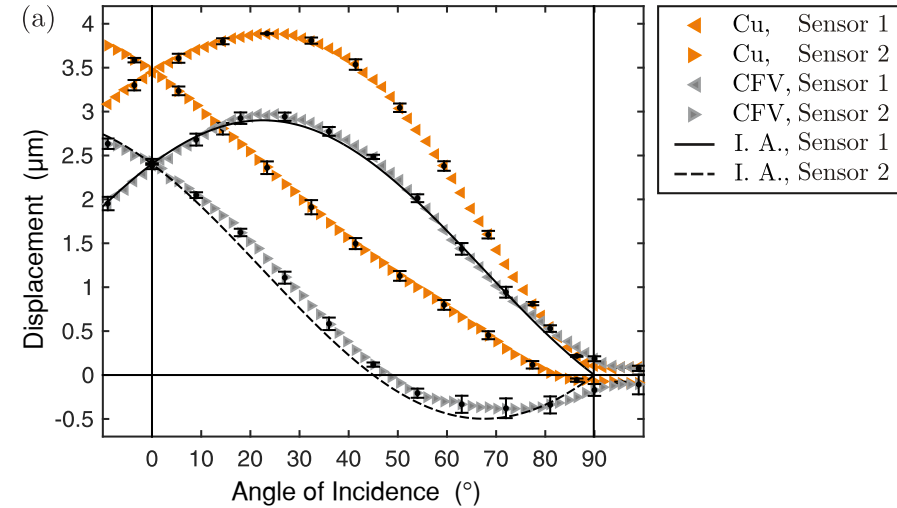


$$F_{\text{normal}} = \sqrt{\frac{1}{2}(F_1 + F_2)}$$

$$F_{\text{in-plane}} = \sqrt{\frac{1}{2}(F_1 - F_2)}$$



Trottenberg et al., EPJ Techn. Instrum. 5, 3 (2018)

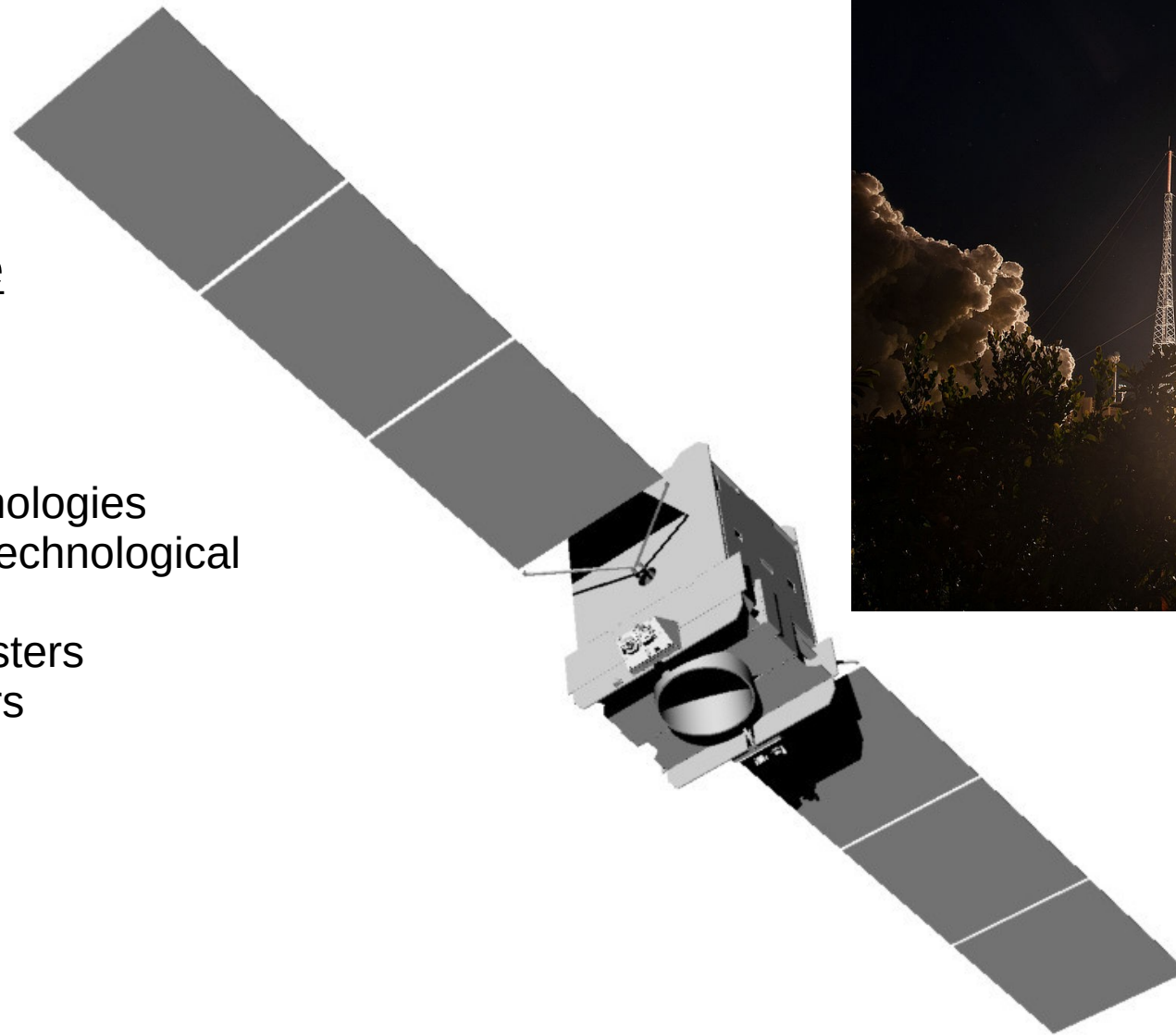


A 1.2 keV Ar/Ar⁺ beam impacts on a copper (Cu) surface and a carbon fiber velvet (CFV) surface. The solid and dashed lines indicate the theoretical case of ideal absorption (I.A.).

The EPDP for the Heinrich Hertz Satellite

Heinrich Hertz Satellite

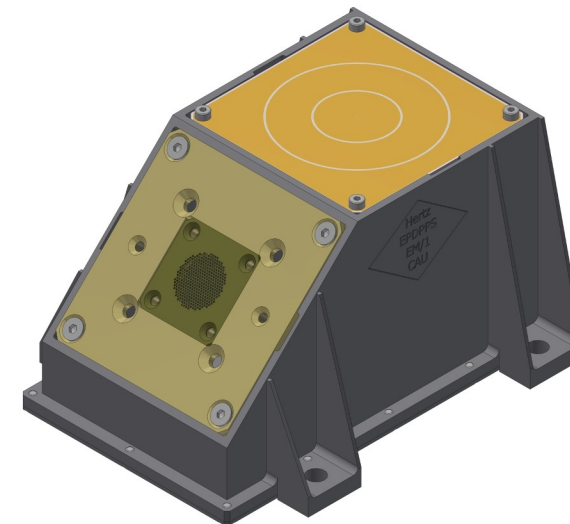
- Explore and test new telecommunications technologies
- Platform for scientific and technological experiments
- Pair of HEMPT 3050 thrusters + pair of SPT-100 thrusters
- launched July 6th, 2023
- Financed by DLR
- Integrated by OHB



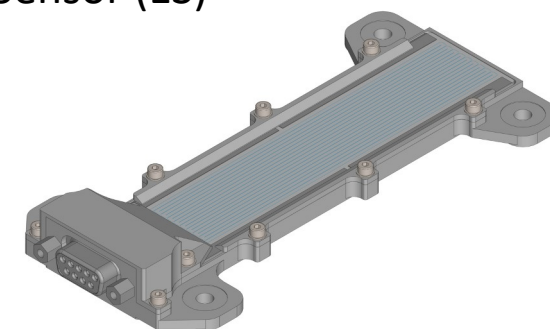
Electric Propulsion Diagnostic Package



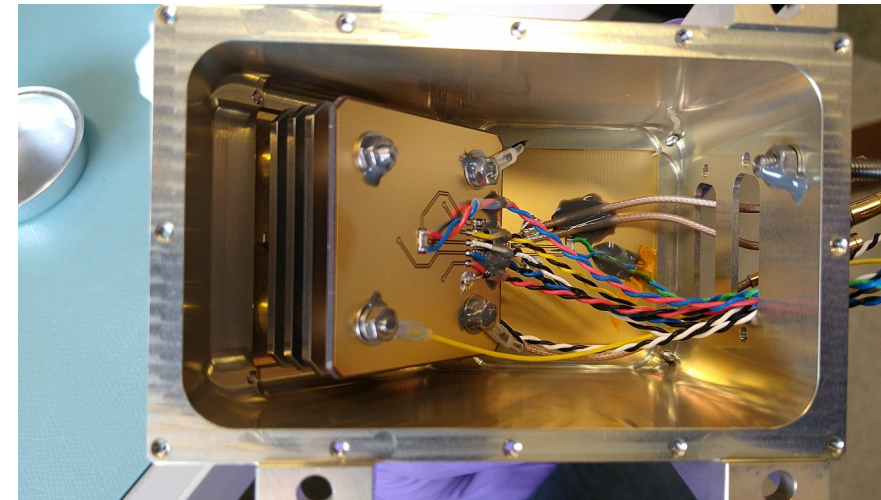
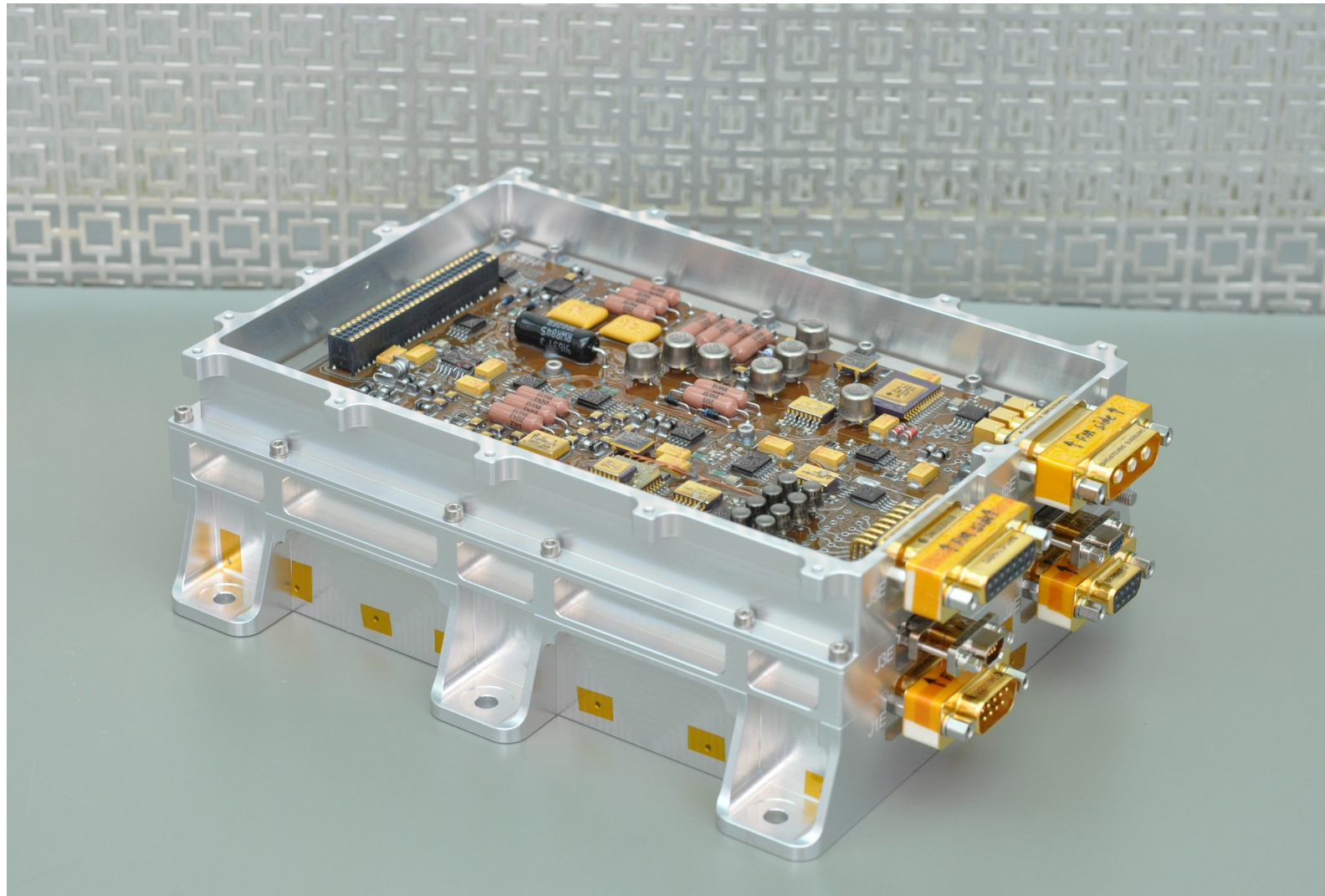
Plasma Sensor (PS)



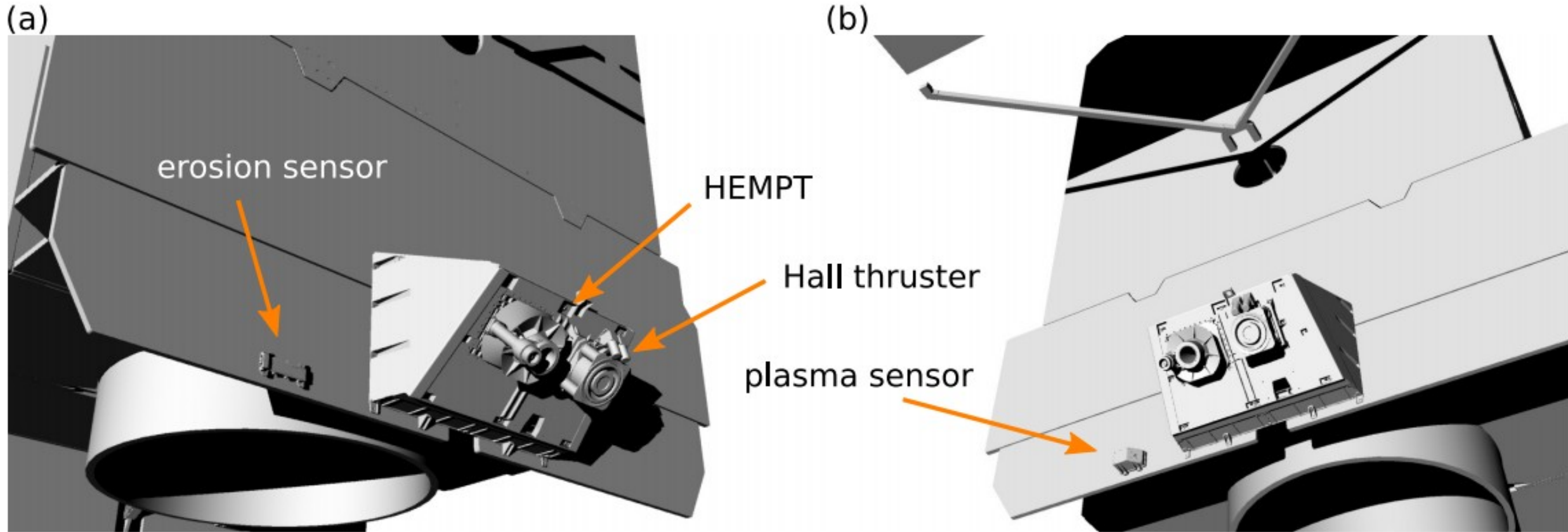
Erosion Sensor (ES)



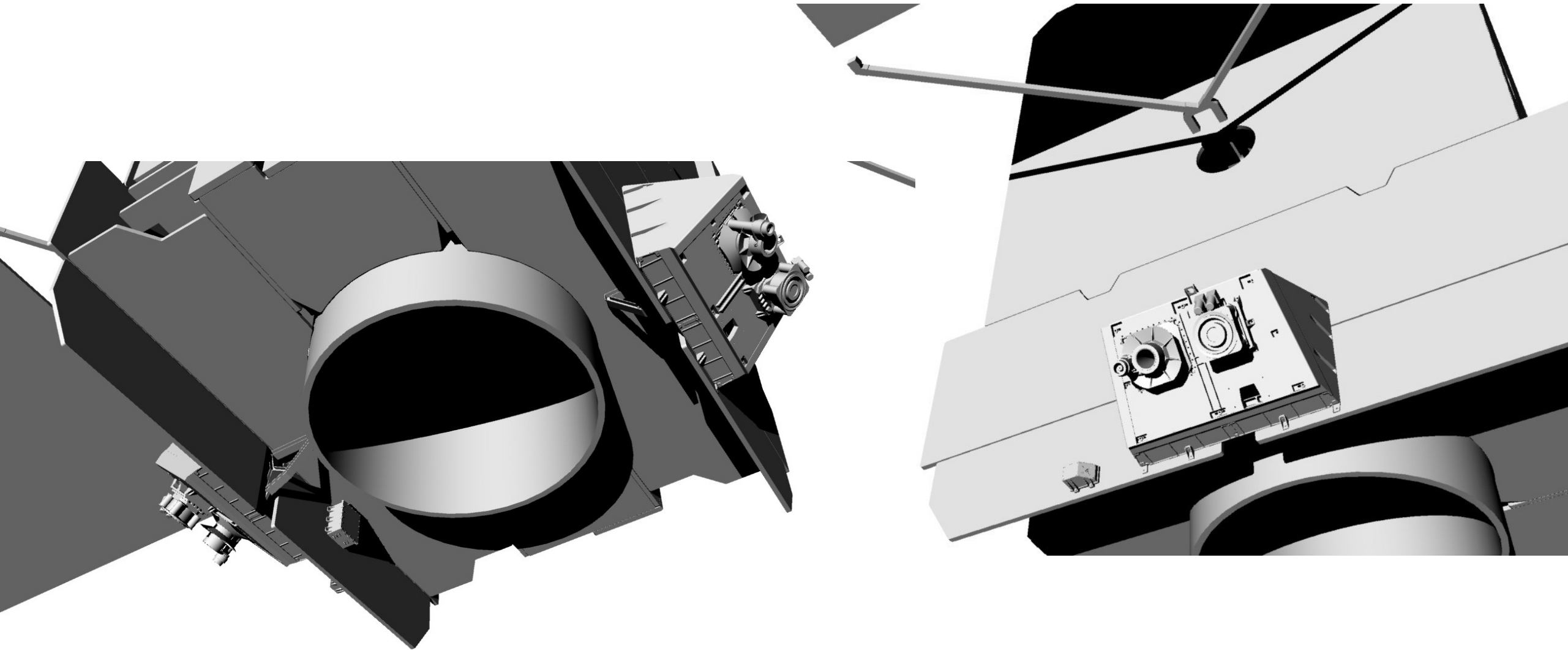
Electric Propulsion Diagnostic Package



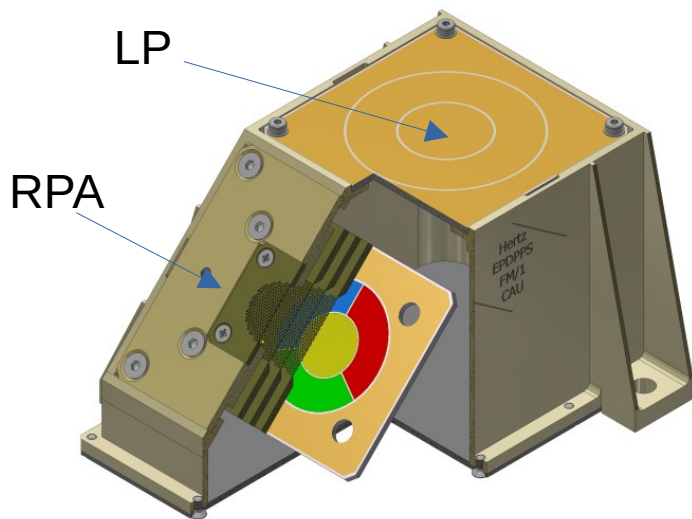
EPDP Mounting Positions on the Satellite



EPDP Mounting Positions on the Satellite

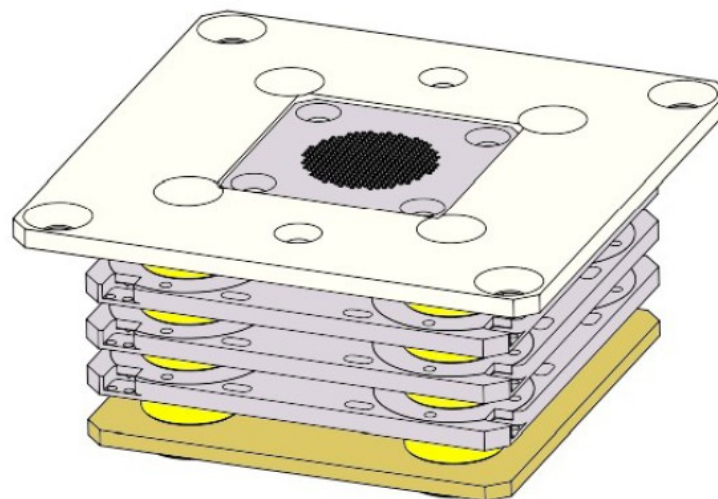


The EPDP Sensors



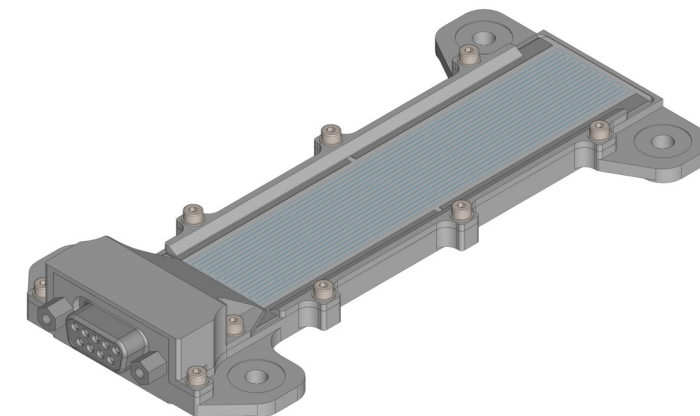
Langmuir Probe (LP):

- Probe area 3.1 cm²
- Ion saturation currents
2 nA ... 0.5 μA



Retarding Potential Analyzer (RPA):

- Four grids
- 0.5 mm holes
- Hexagonal pattern
- 0.7 mm “grid constant”
- Segmented collector
- 23 mm entrance to collector



Erosion Sensor:

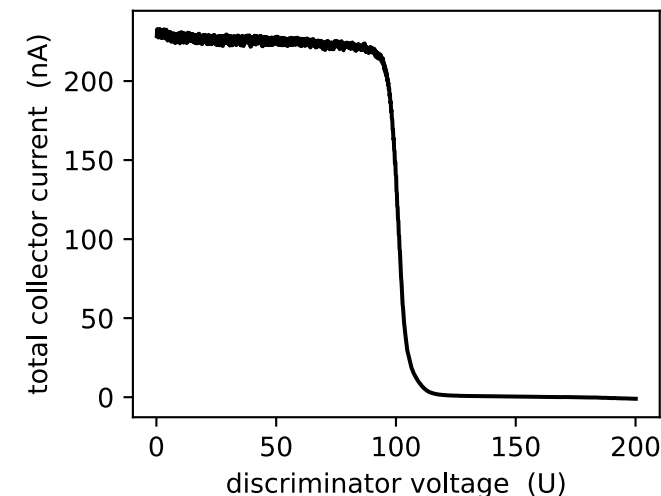
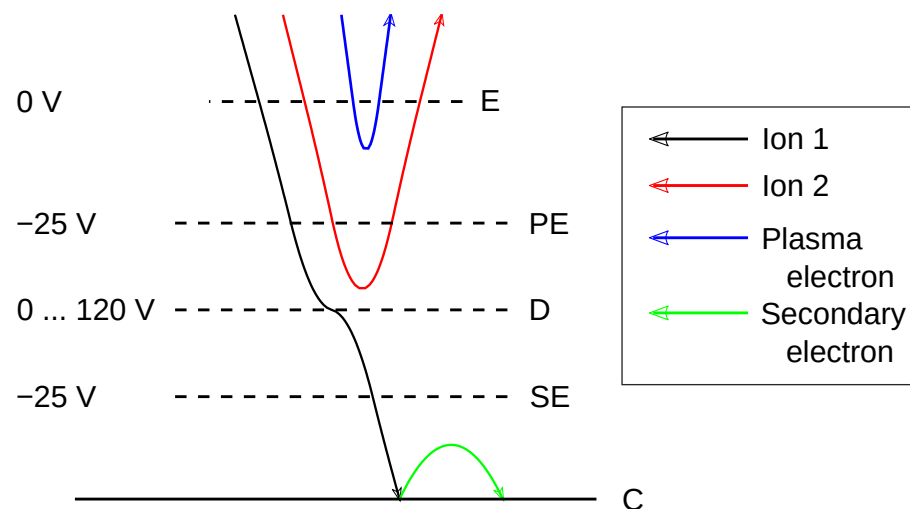
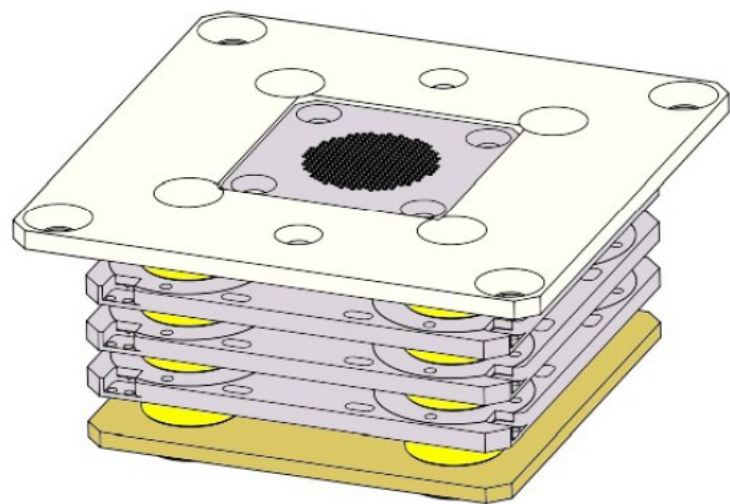
Resistance measurement

Silver meander on ceramic
originally 15 Ω:

- 180 cm long
- 2 μm thick
- 1 mm wide

Trottenberg et al., EPJ Techn. Instrum. 8, 16 (2021)

Quick Recap: What is a Retarding Potential Analyzer (RPA)?



Four-grid RPA

- E: Entrance grid
- PE: Plasma electron repeller grid
- D: Discriminator grid
- SE: Secondary electron repeller grid
- C: Collector

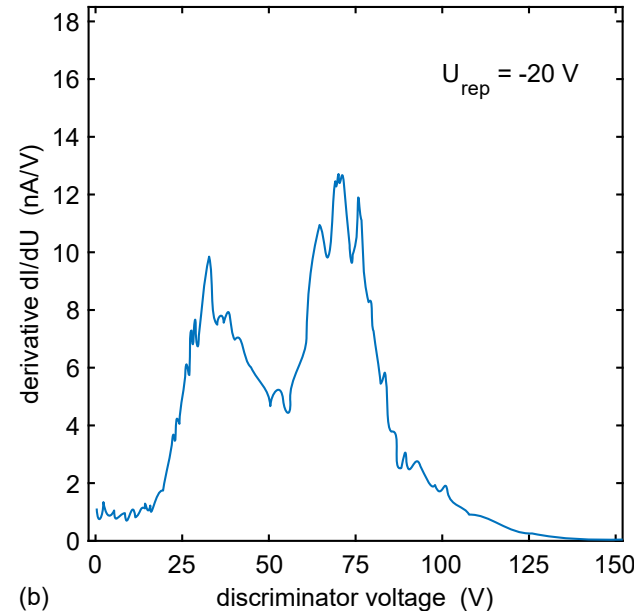
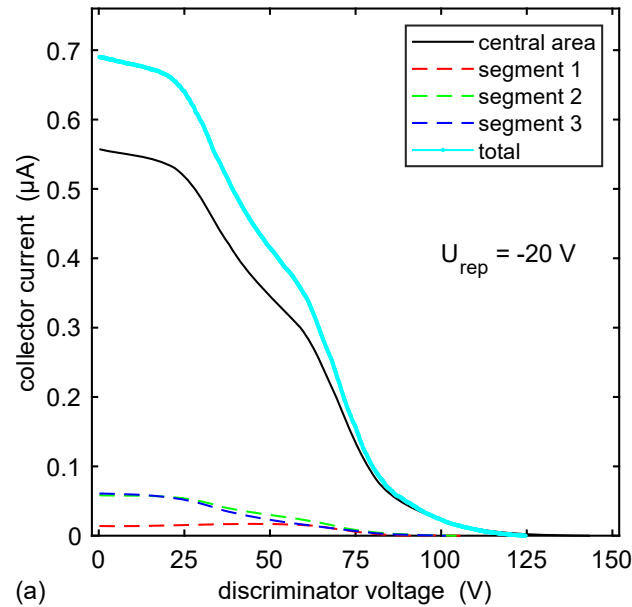
The trajectories illustrate...

- an ion (black) that overcomes the retarding potential,
- one that does not (red),
- electrons originating from the plasma (blue),
- electrons from the collector (green).

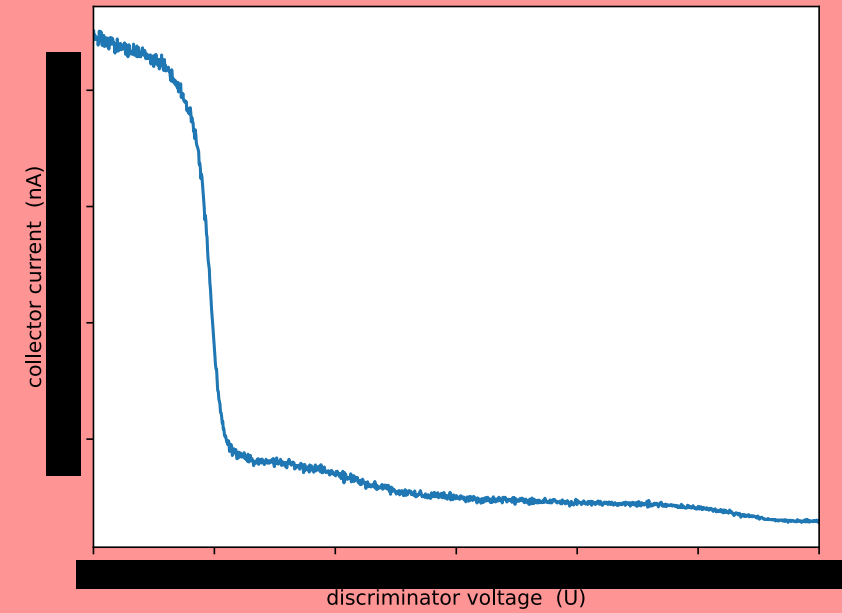
- Characteristics are monotonically decreasing
- Derivatives yield distribution functions

Data from Measurements with a HEMPT: Chamber & Space

Data from Tests in ULAN chamber (Thales)

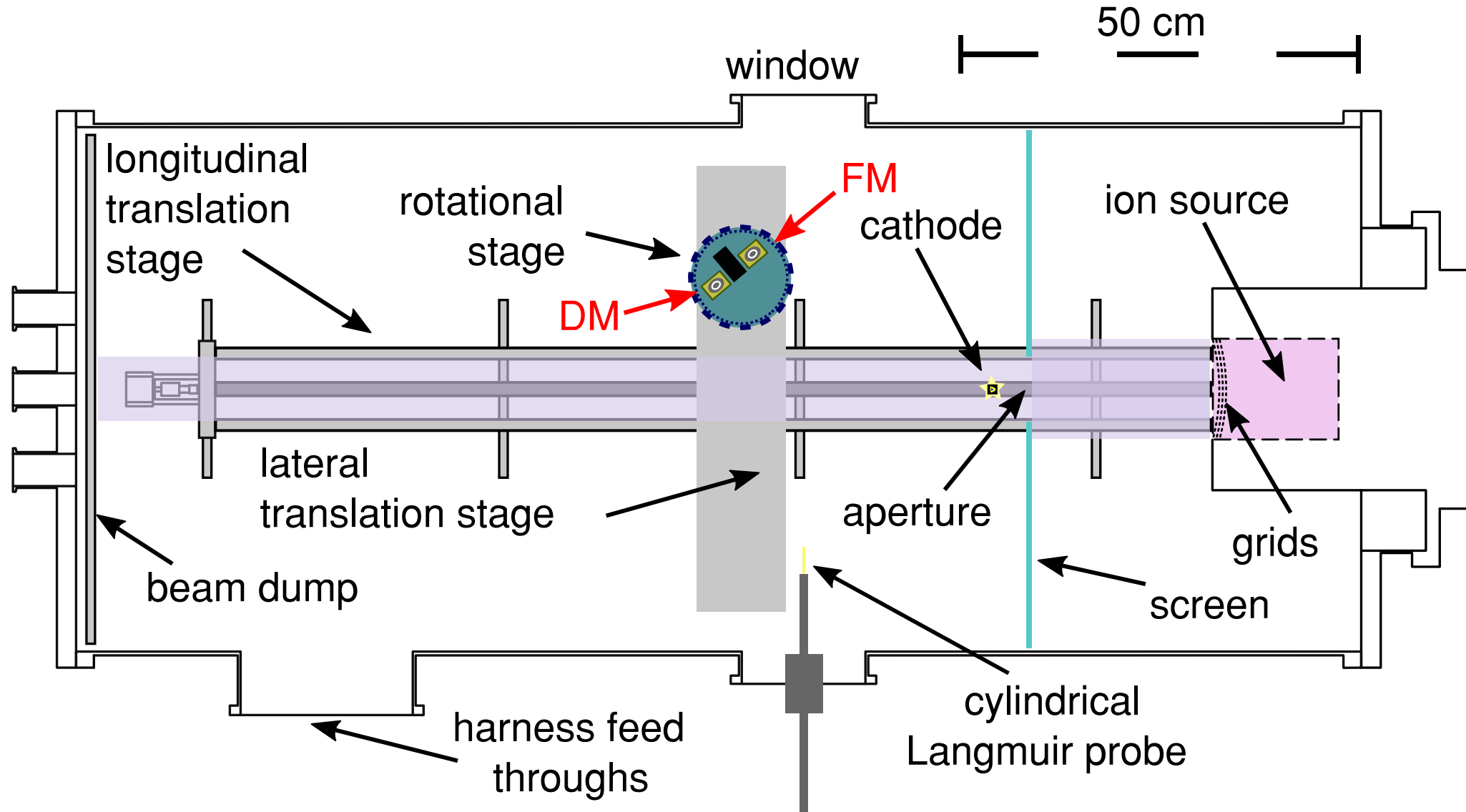


Data from EPDP in Space
(absolute values not disclosed)

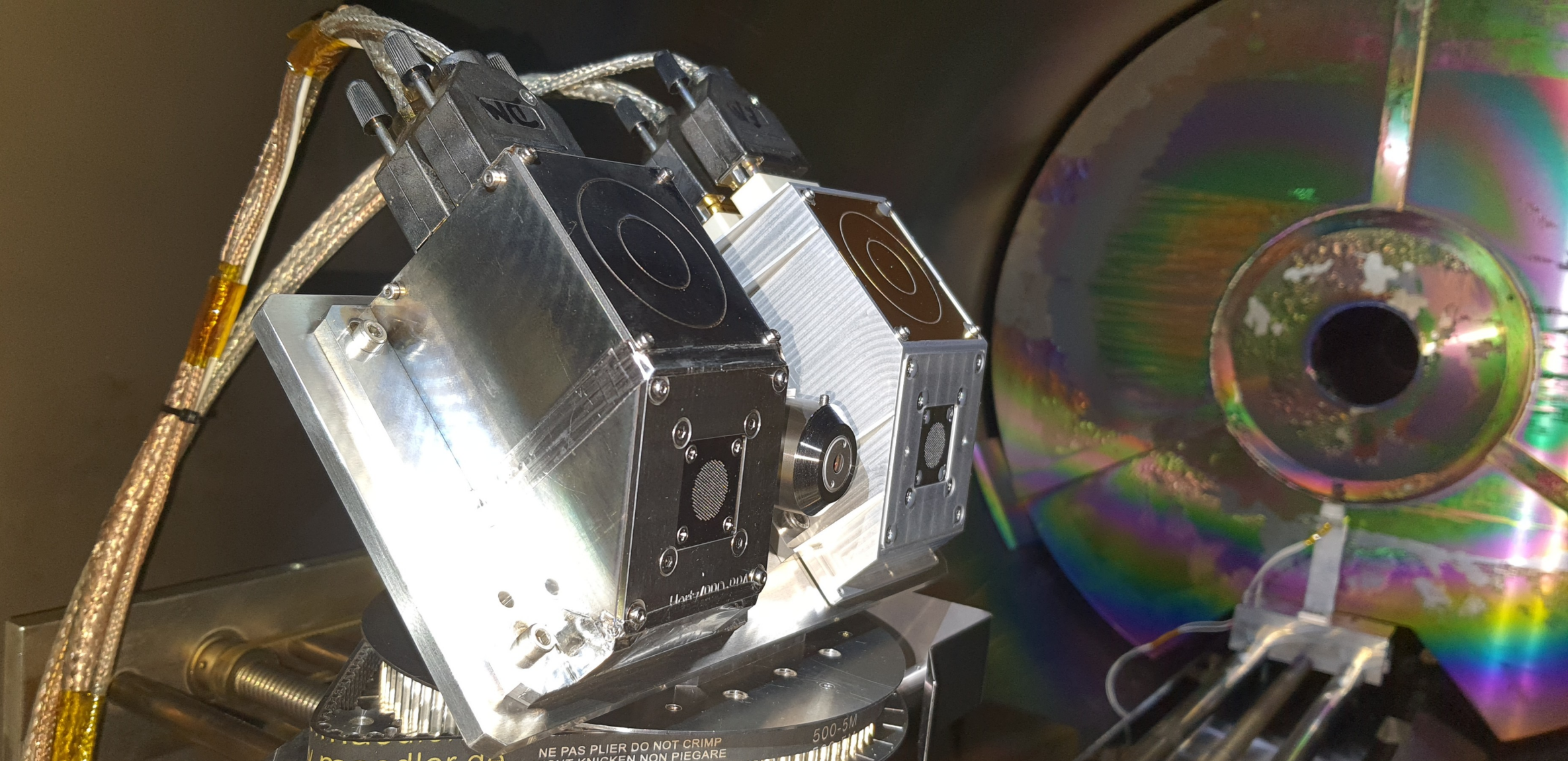


Data from the Plasma Sensor

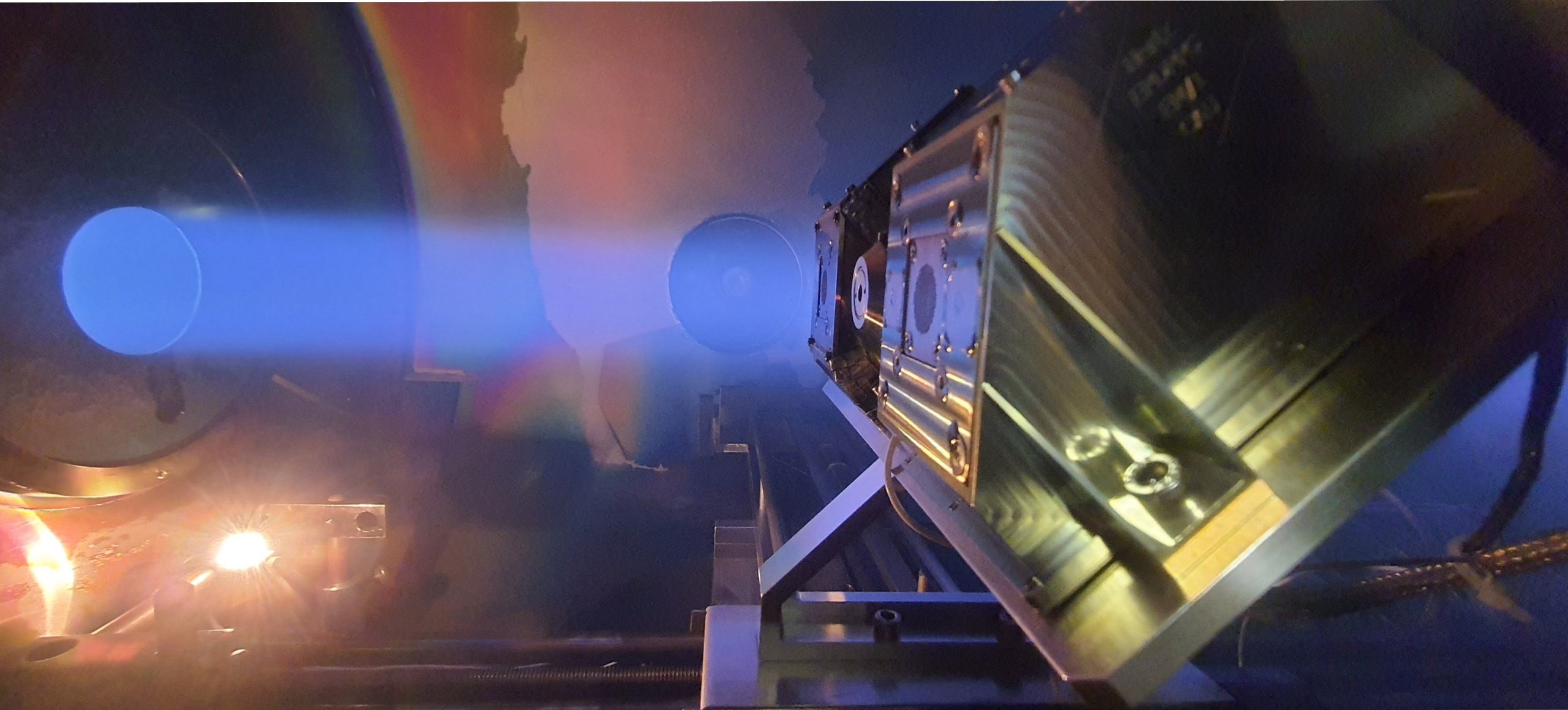
Test Setup for Mimicking the Secondary Plasma from the Thruster



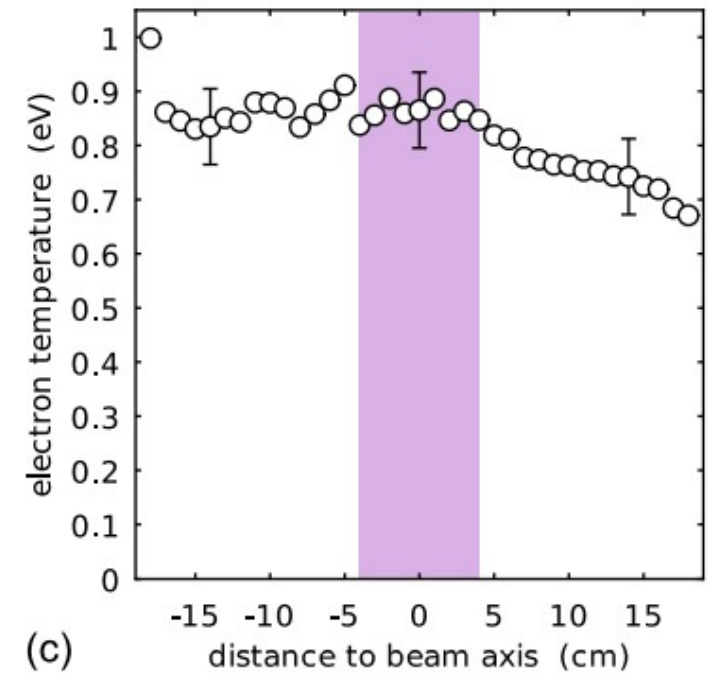
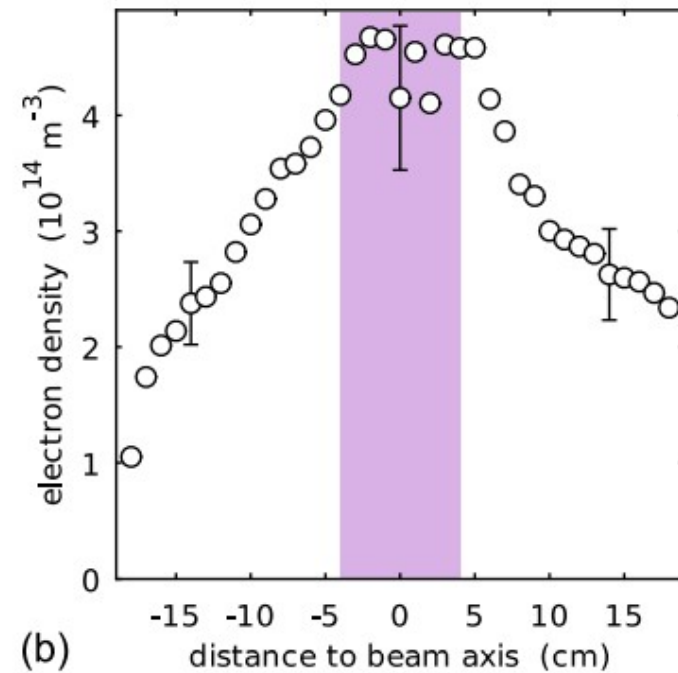
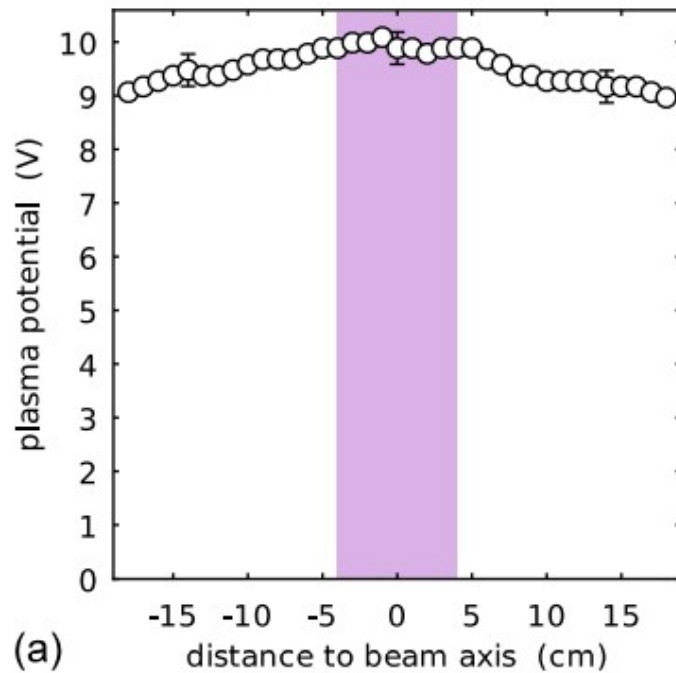
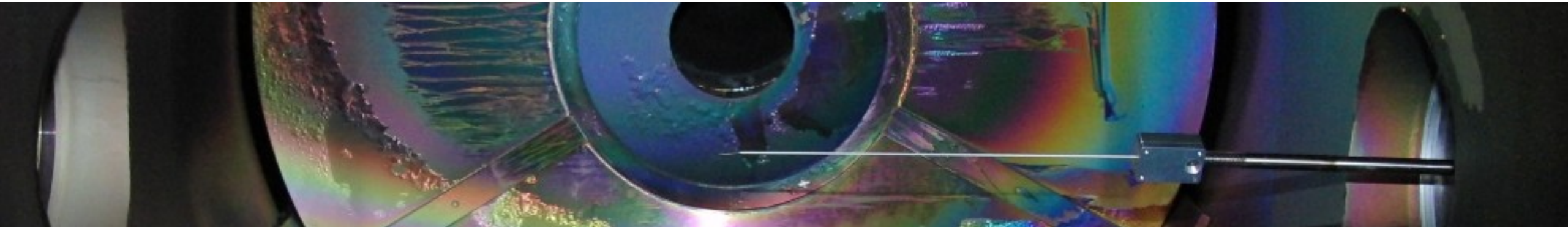
Test Setup with two Prototypes of the Plasma Sensor



Test Setup with Xenon Ion Beam

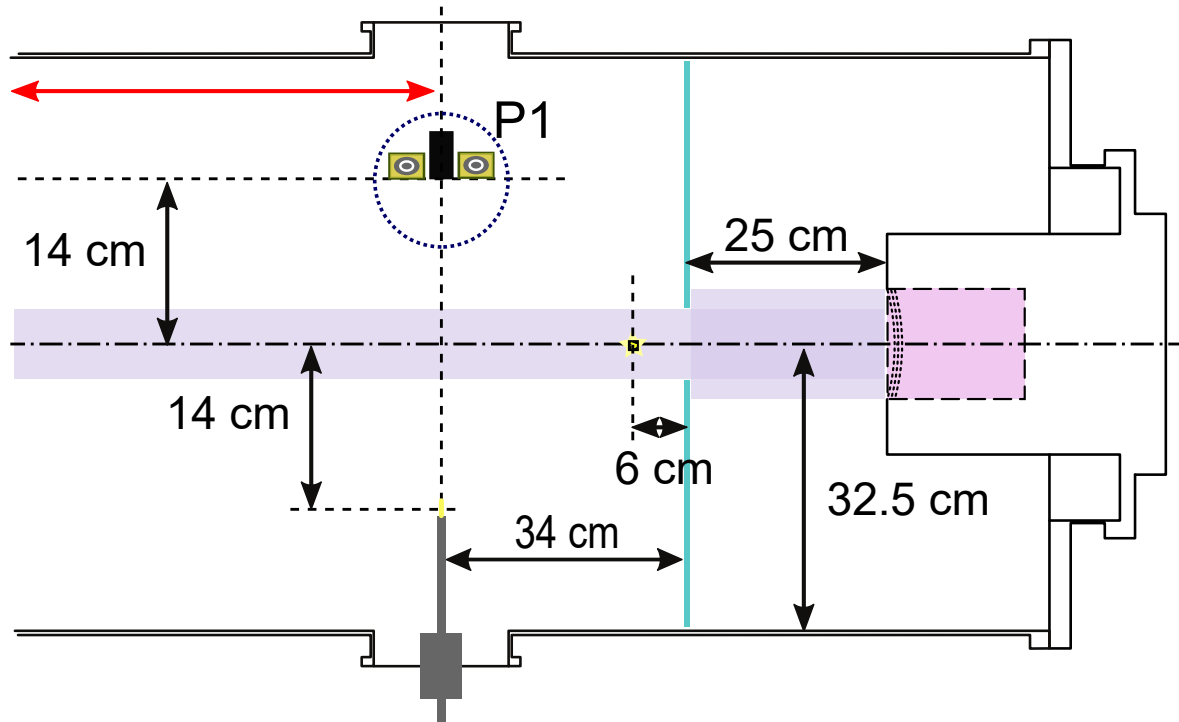


Test Setup: Plasma Diagnostics in the Chamber with Xenon Ion Beam



Trottenberg et al., EPJ Techn. Instrum. 8, 16 (2021)

Test Setup: Controlled Generation of CEX Ions with Different Energies

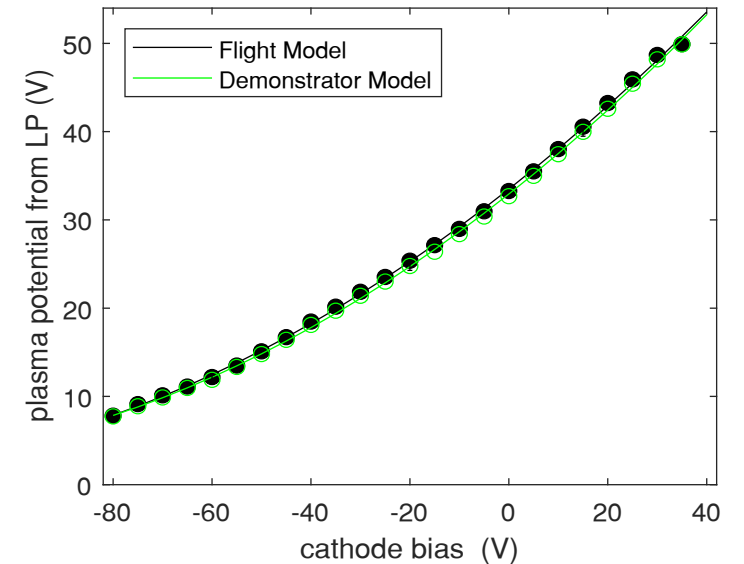


The cathode is biased in the range $-80\text{ V} \dots +20\text{ V}$.



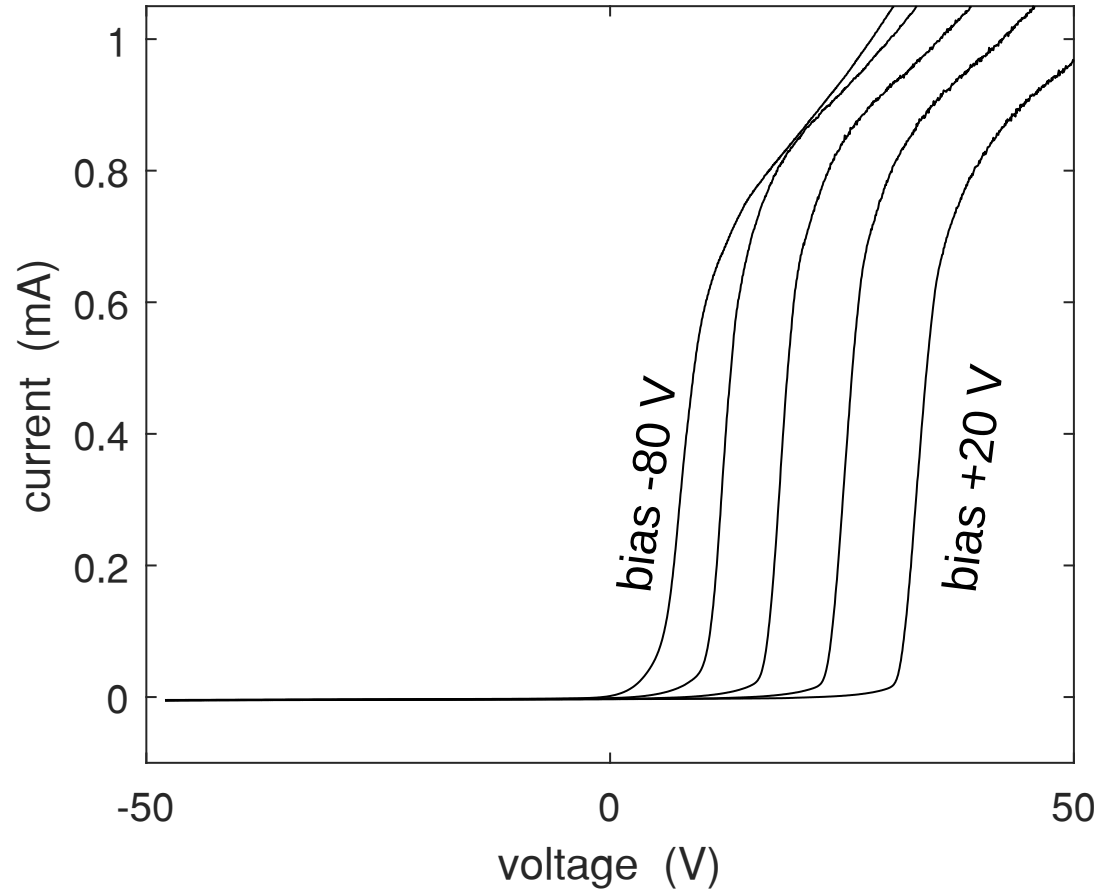
The plasma potential varies from $\sim 10\text{ V}$ to $\sim 50\text{ V}$.

- Position of the sensors: outside the 1.2-keV beam
- Biasing the cathode shifts the plasma potential
- Purpose: Different energies can be given to the CEX ions.

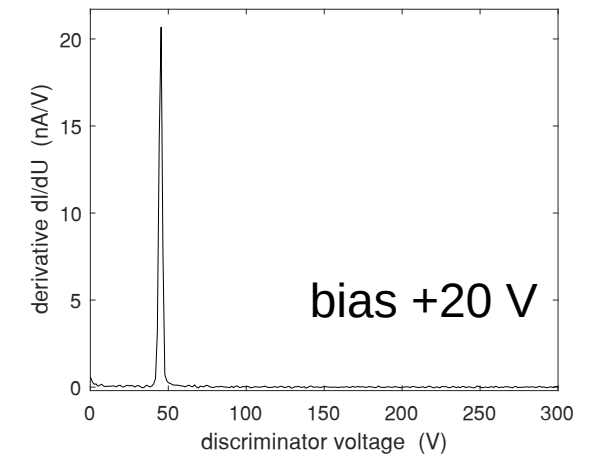
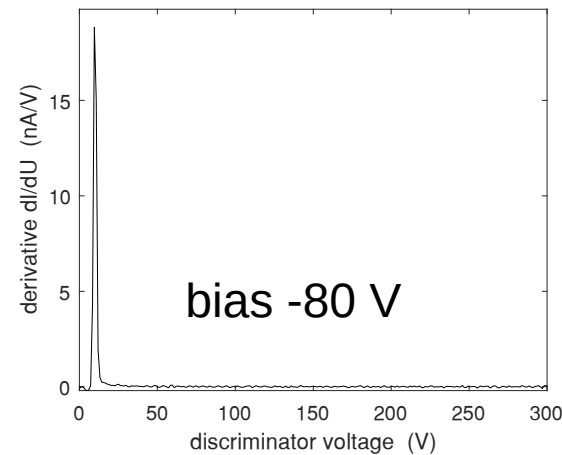
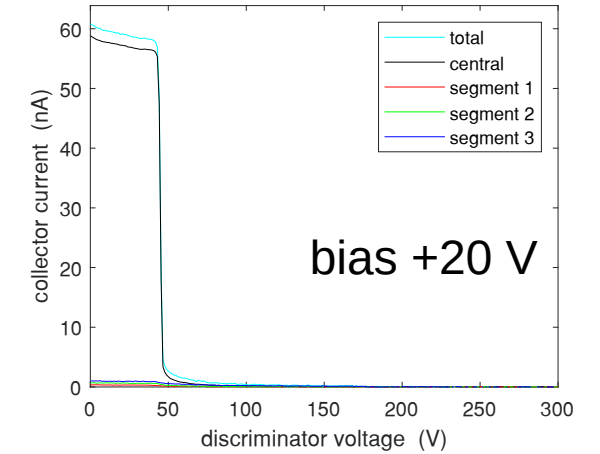
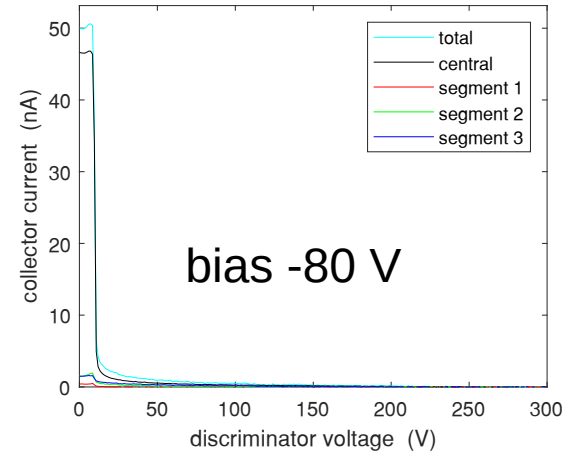


Test Setup: Controlled Generation of CEX Ions with Different Energies

LP: measured 14 cm away from the beam
for $U_{\text{cath}} = -80 \text{ V}, -60 \text{ V}, -40 \text{ V}, -20 \text{ V}, 0 \text{ V}$



RPA: measured 14 cm away from the beam
for $U_{\text{cath}} = -80 \text{ V}, +20 \text{ V}$.



Test Setup with “Idling” Ion Beam Source: Ion energies ~100 eV

Ranges of the Plasma Sensor:

Energy: 0 – 300 eV

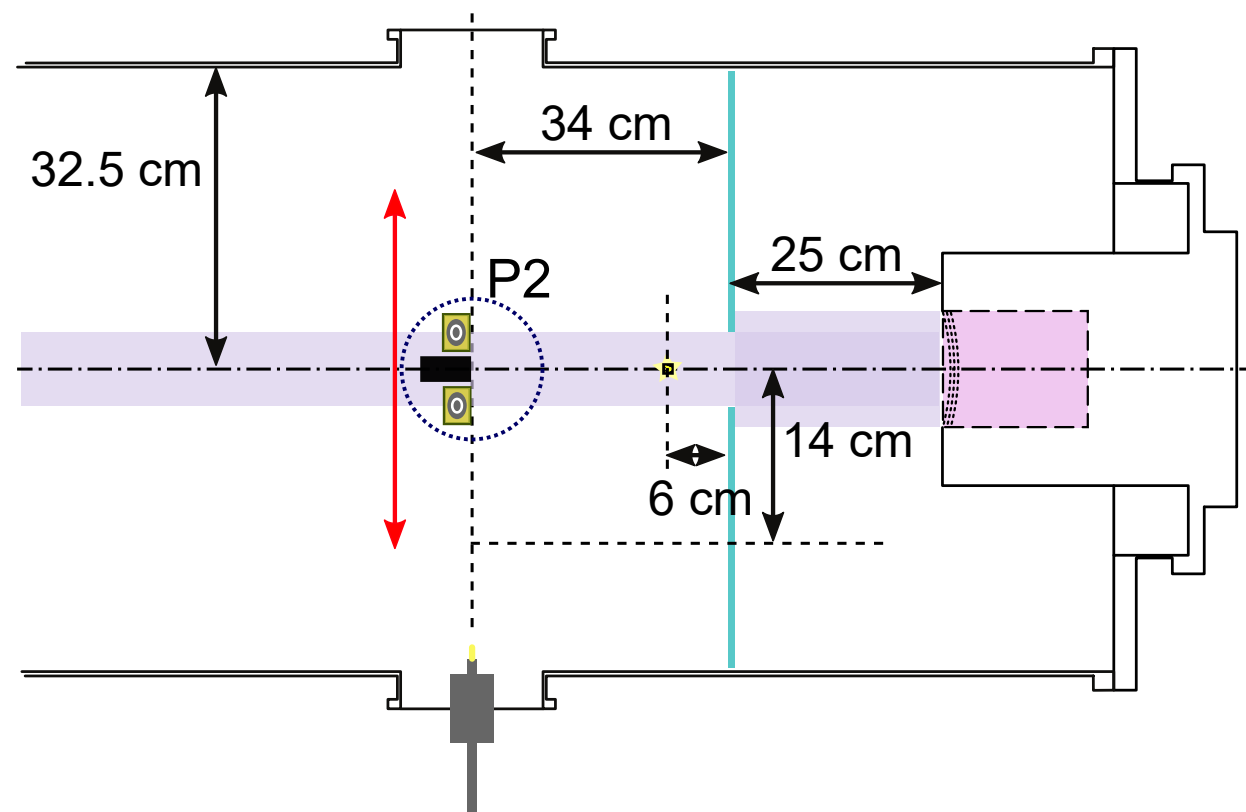
Collector currents: < 1 μ A

Cannot be exposed to 1,2-keV beam

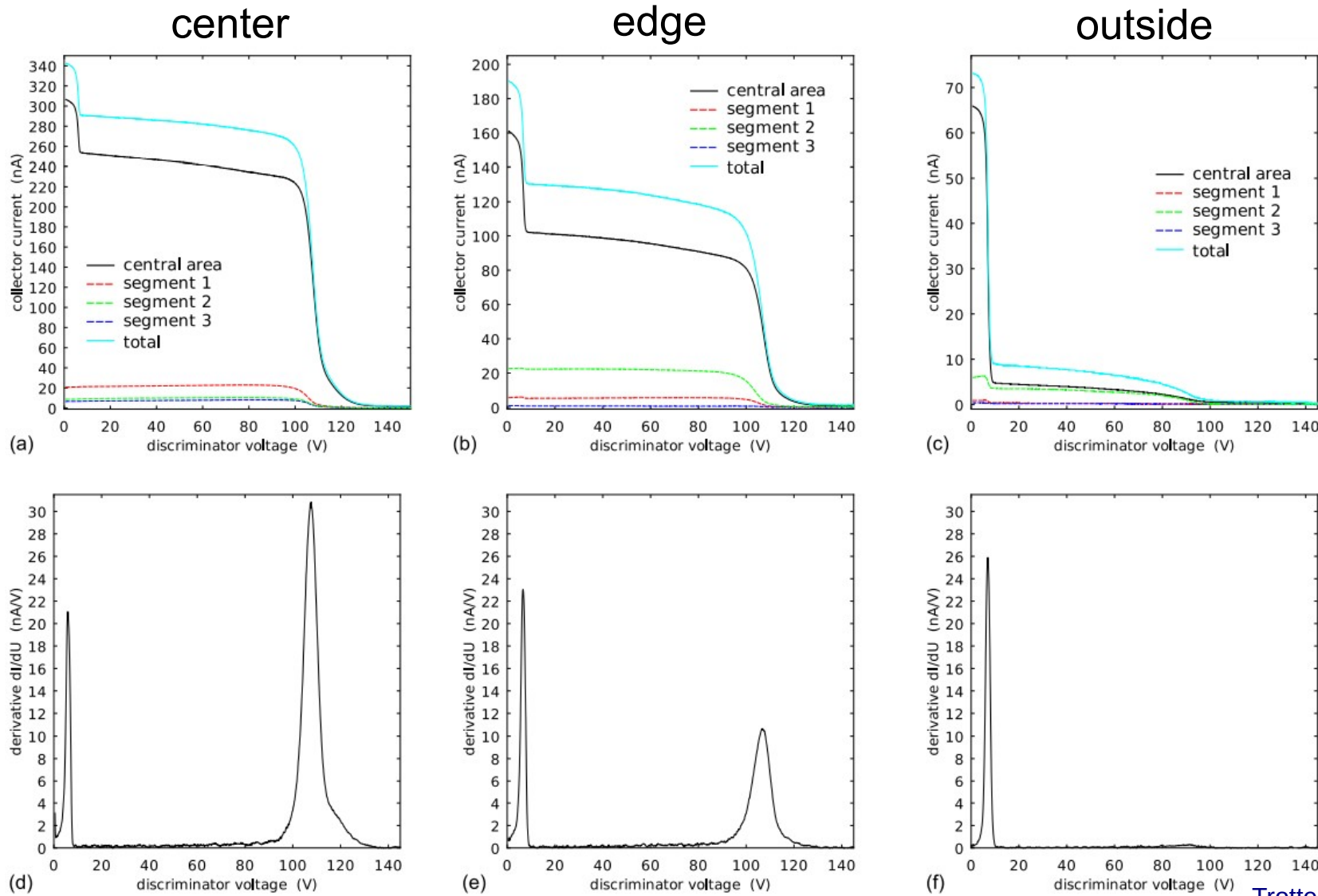
Operating the ion source without acceleration (anode) voltage:

Ion energy: ~ 100 eV

Ion current density: 17.3 mA/m²



Test Setup with “Idling” Ion Beam Source: Ion energies ~100 eV



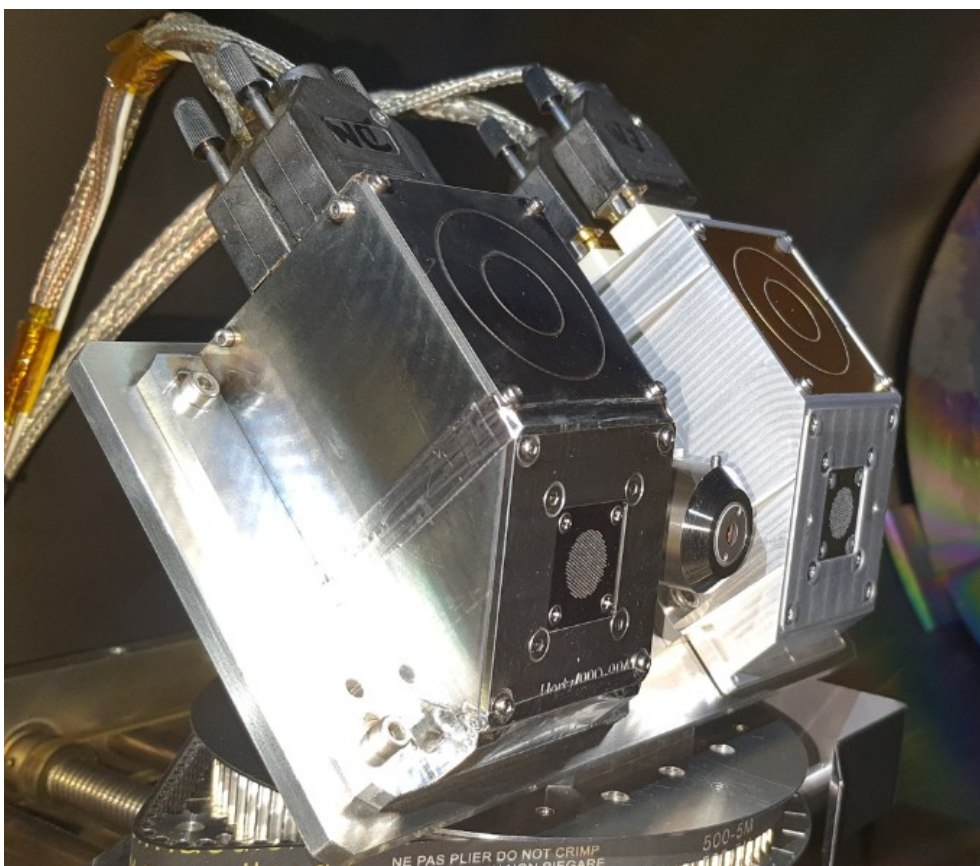
RPA characteristics and derived energy distributions at three positions relative to the beam.

- Two populations:
- Primary ions
 - Charge-exchange ions

Trottenberg et al., EPJ Techn. Instrum. 8, 16 (2021)

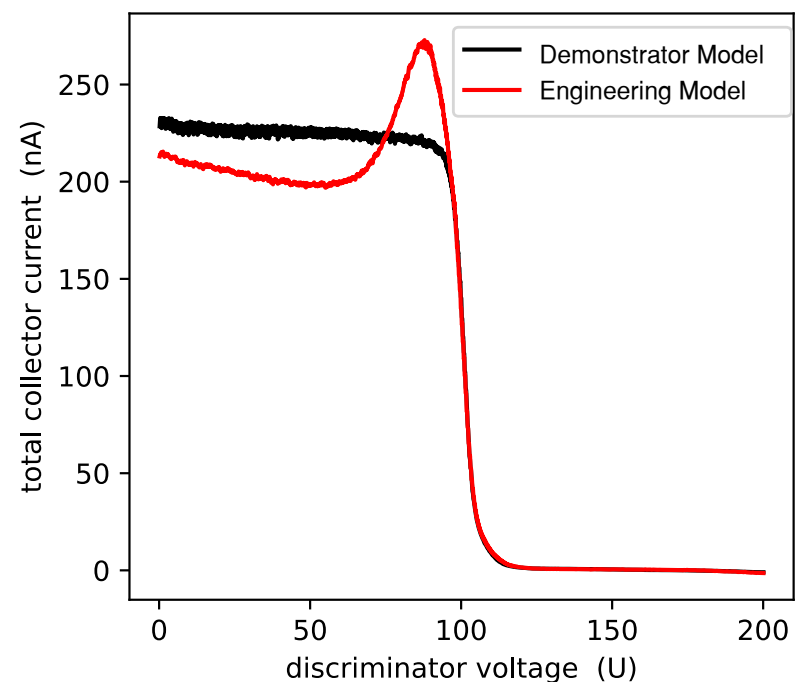
Unexpected Features of the Retarding Potential Analyzer

A Surprising Anomalie in the Characteristic of the EM

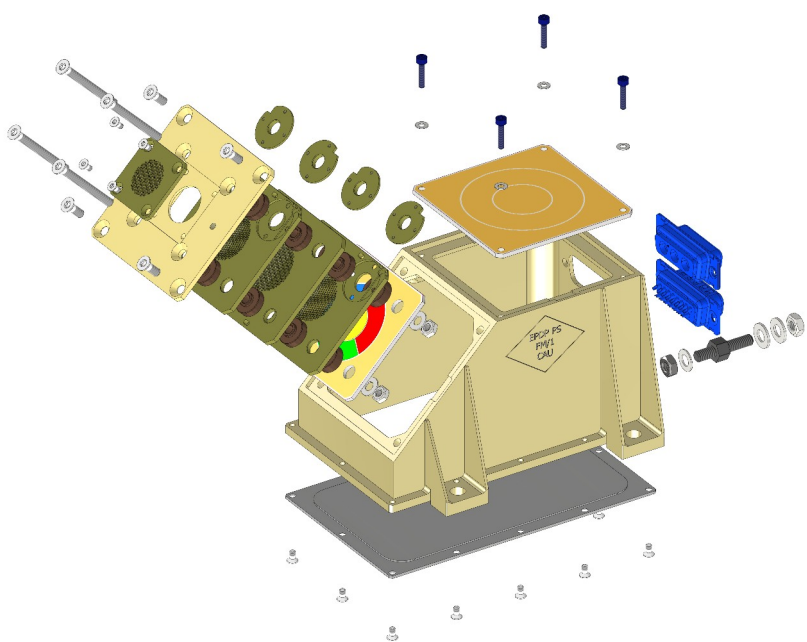


The ‚Demonstrator Model‘ and the later built Engineering Model‘ produced significantly different trajectories – What happened?

A “good” characteristic should be monotonically decreasing!

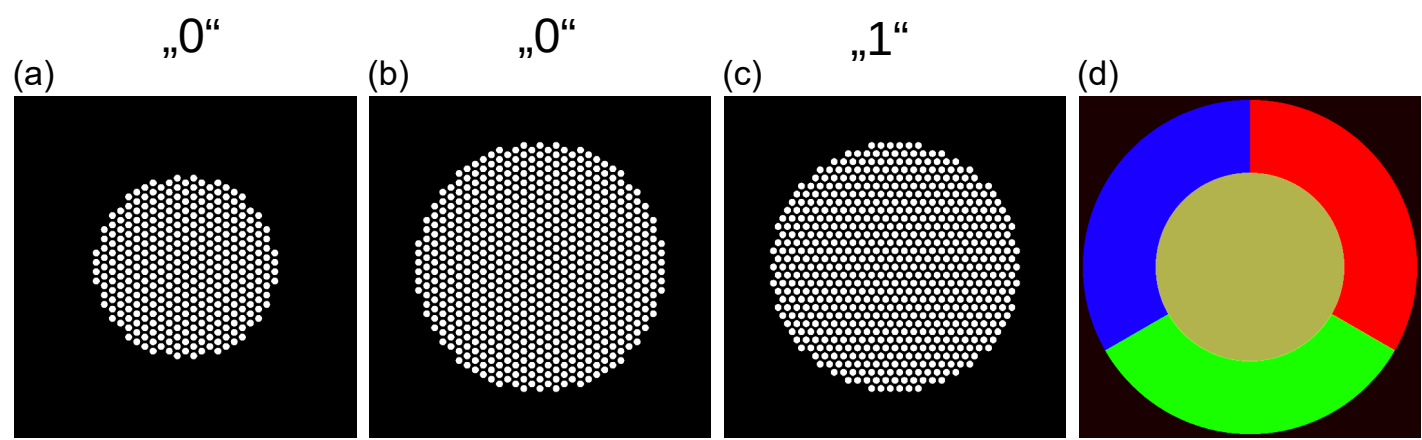


Grid Orientations



The hexagonal pattern and the square frames allow two different orientations of each grid: *rotated* or *not rotated*.

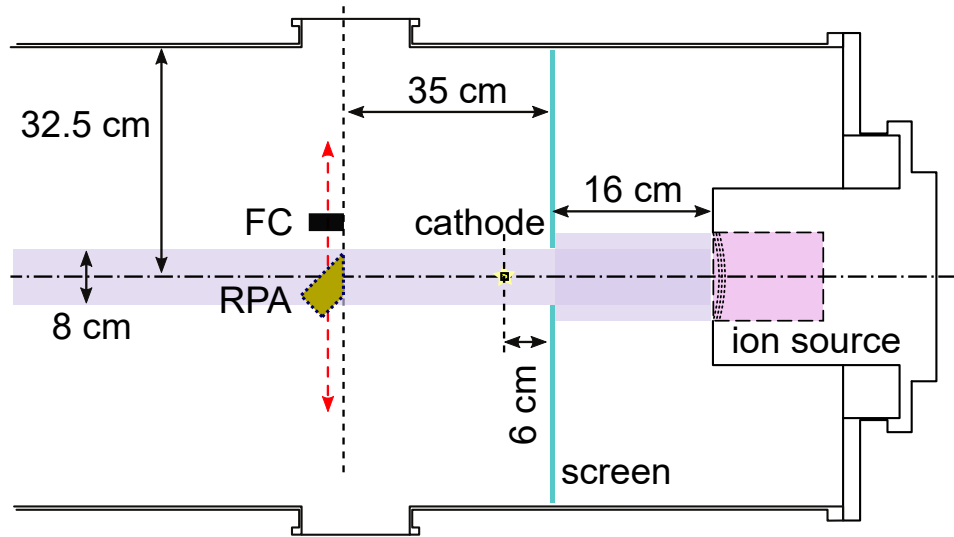
0: not rotated
1: rotated



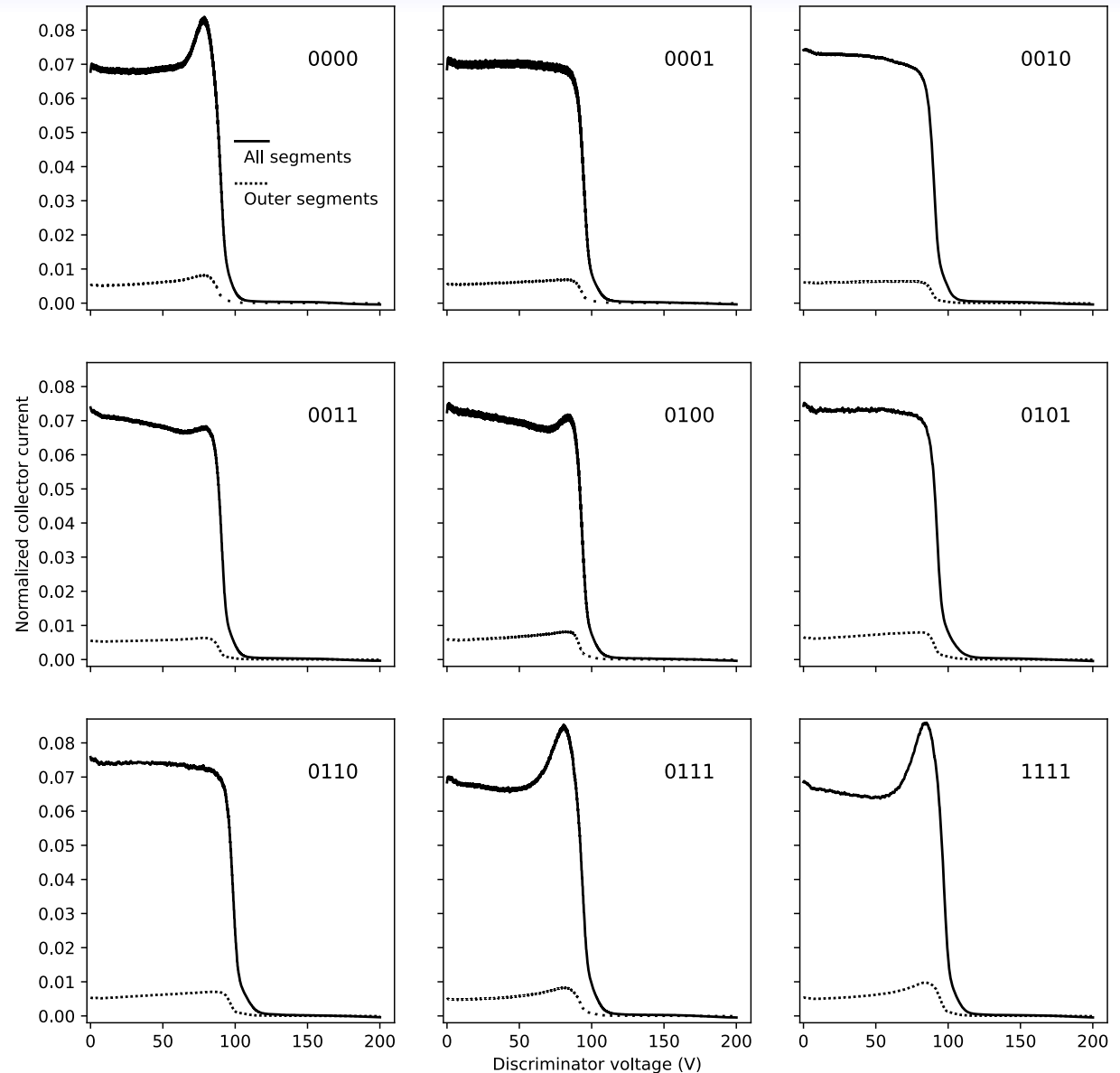
	0000
	0001
	0010
	0011
	0100
	0101/ "DM"
	0110
	0111
	1111/ "EM"

Grid Orientations

Setup:



RPA characteristics (I vs V)



We operated the ion source without applying an acceleration voltage („idling mode“)

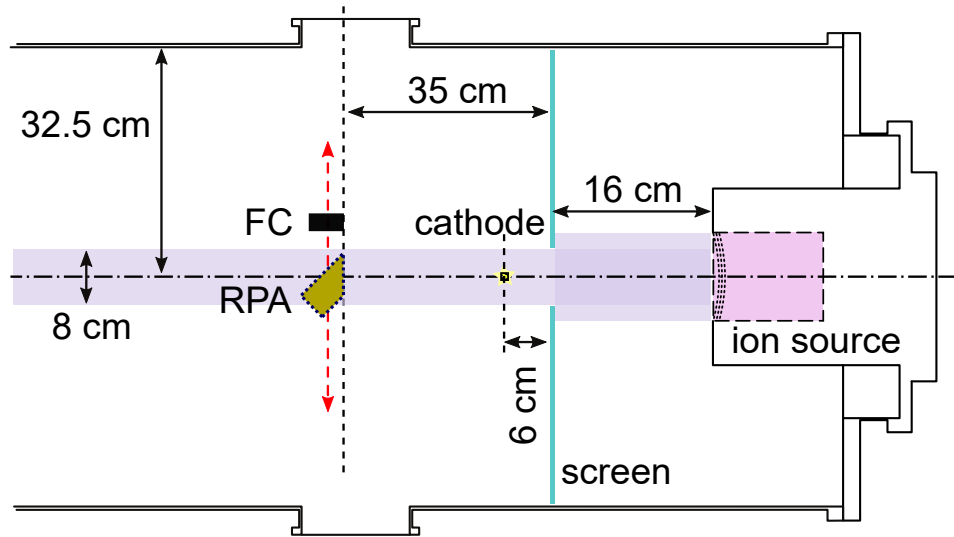
→ ion energies: ~100 eV,
low current densities: ~17 mA/m².

The RPA was reconfigured 8 times.

Trottenberg et al., AIP Advances 15, 035030 (2025)

Grid Orientations

Setup:



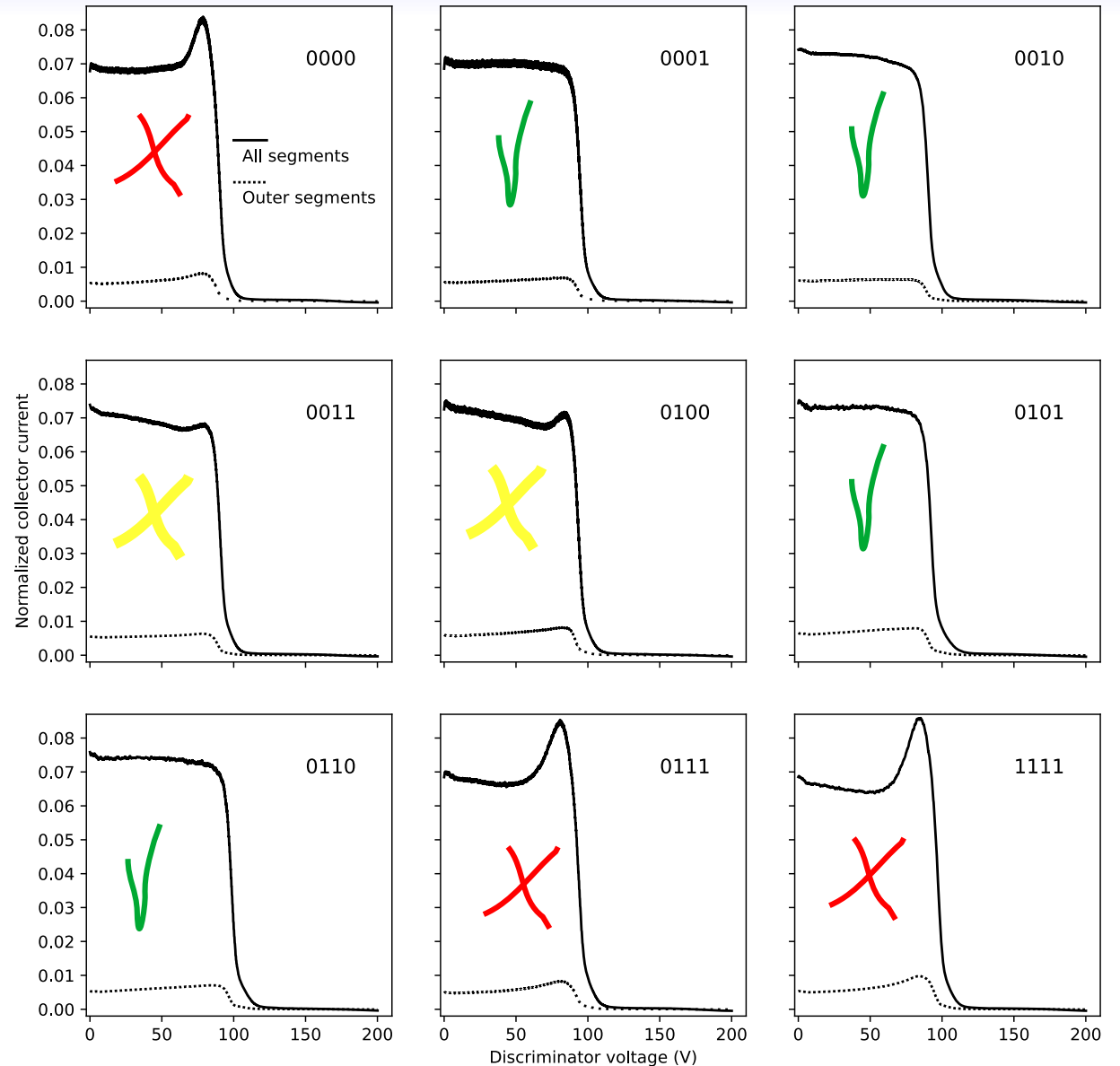
We operated the ion source without applying an acceleration voltage („idling mode“)

→ ion energies: ~100 eV,
low current densities: ~17 mA/m².

The RPA was reconfigured 8 times.

Trottenberg et al., AIP Advances 15, 035030 (2025)

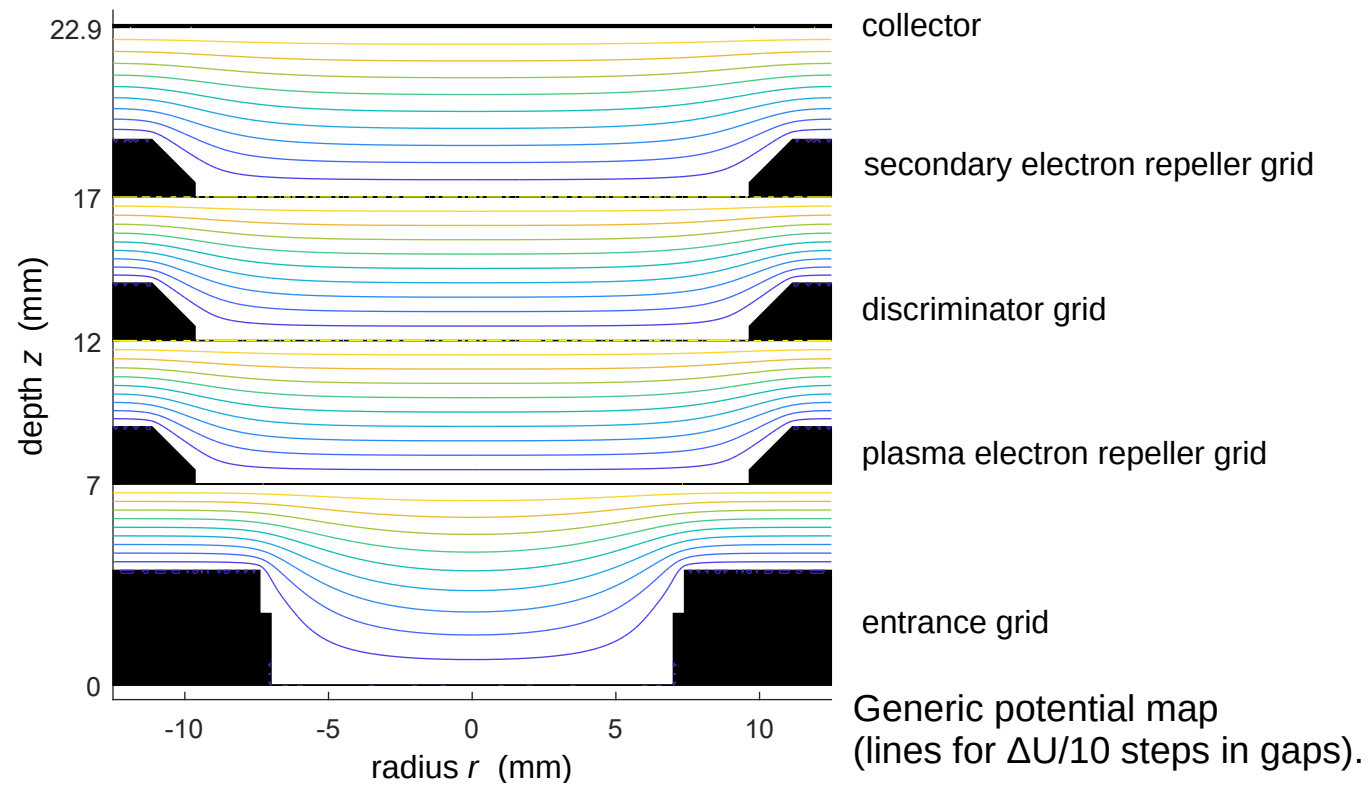
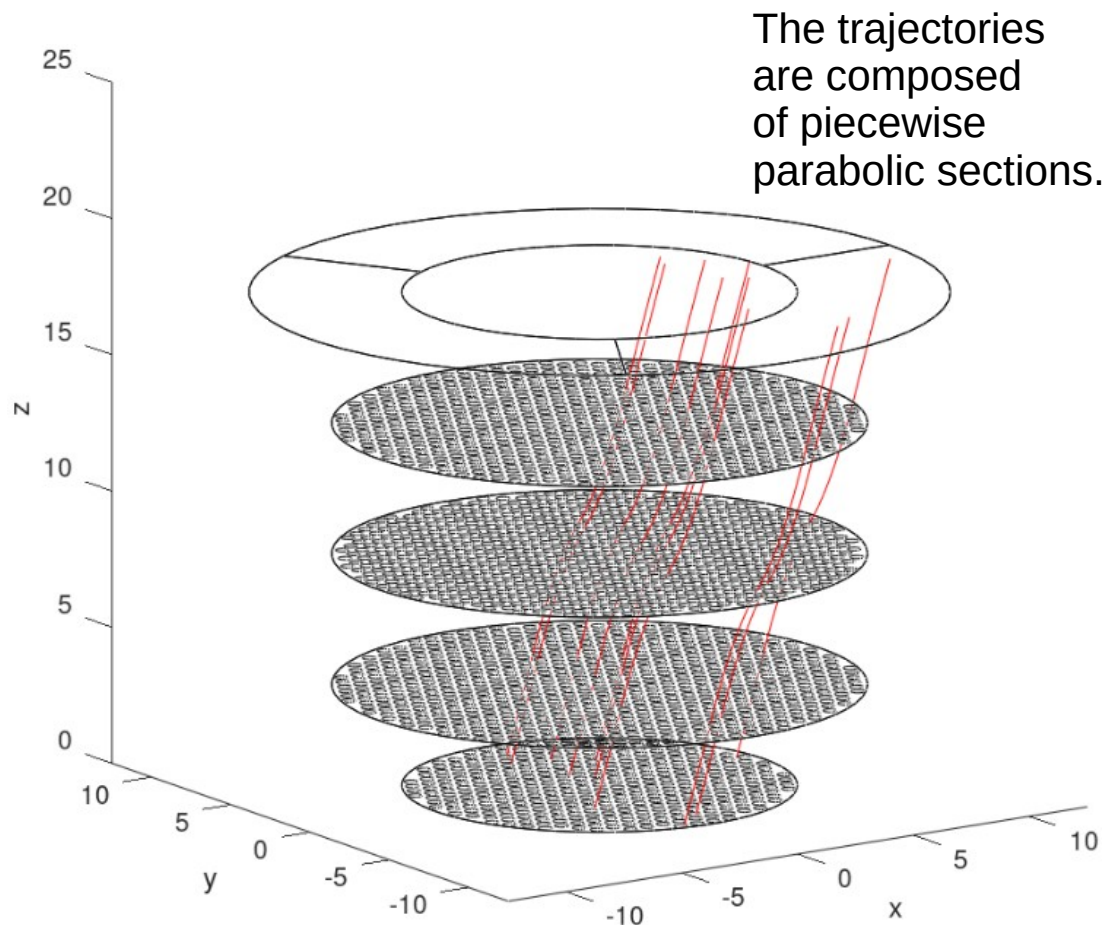
RPA characteristics (I vs V)



Modeling of the Retarding Potential Analyzer

The simplest model assumes homogeneous electric fields between the grids

An improved model accounts for field distortions due to the 3d structure of the grid frames

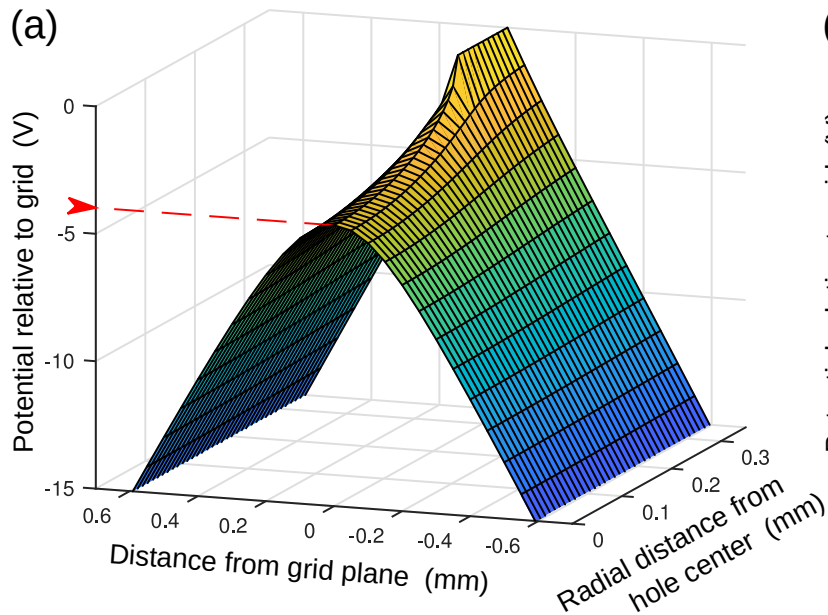


Trottenberg et al., AIP Advances 15, 035030 (2025)

Modeling of the Retarding Potential Analyzer

Further refinements: Near-field effects in the holes.
 The grid with holes may be either thin or of finite thickness.

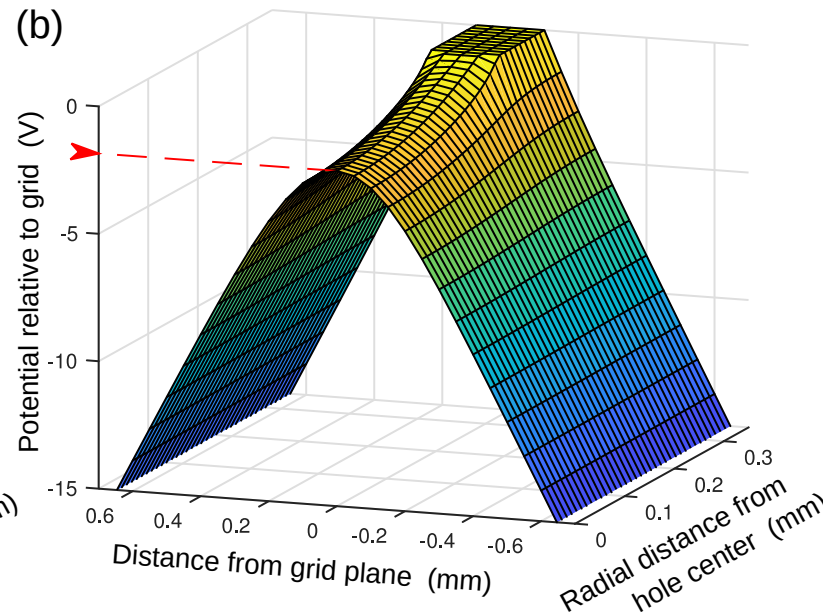
Thin grid



Analytical solution

Jackson, Classical Electrodynamics, 3rd. ed. (1999)

Thick grid (200 μm)



Finite Element Method

Shown Example:
 Repeller grids at -25 V,
 discriminator grid at +100 V.

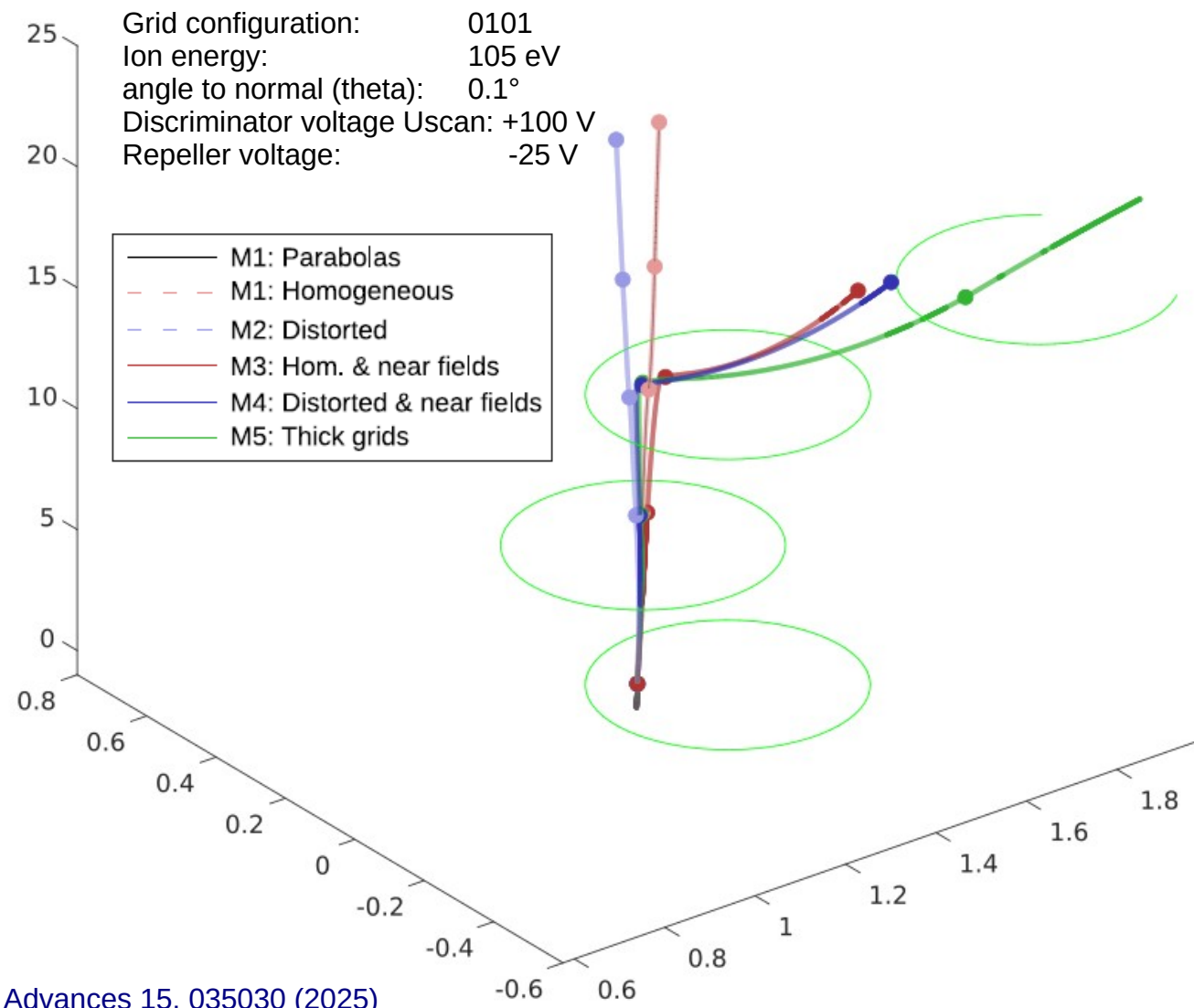
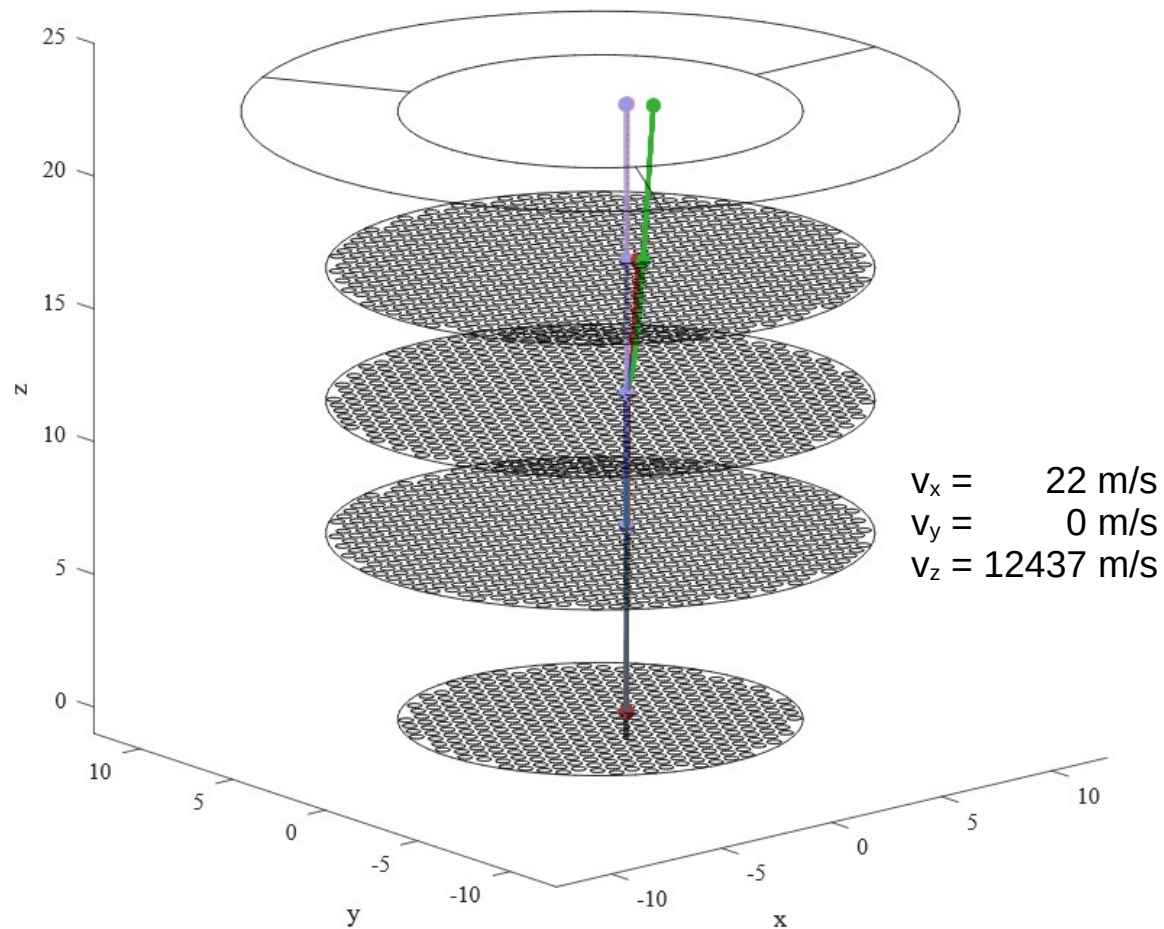
Saddle point potentials:
 (a) -3.98 V below grid potential,
 (b) -1.85 V below grid potential.

Consequence of the saddle points:
 „too slow“ ions can pass through the discriminator grid.

Trottenberg et al., AIP Advances 15, 035030 (2025)

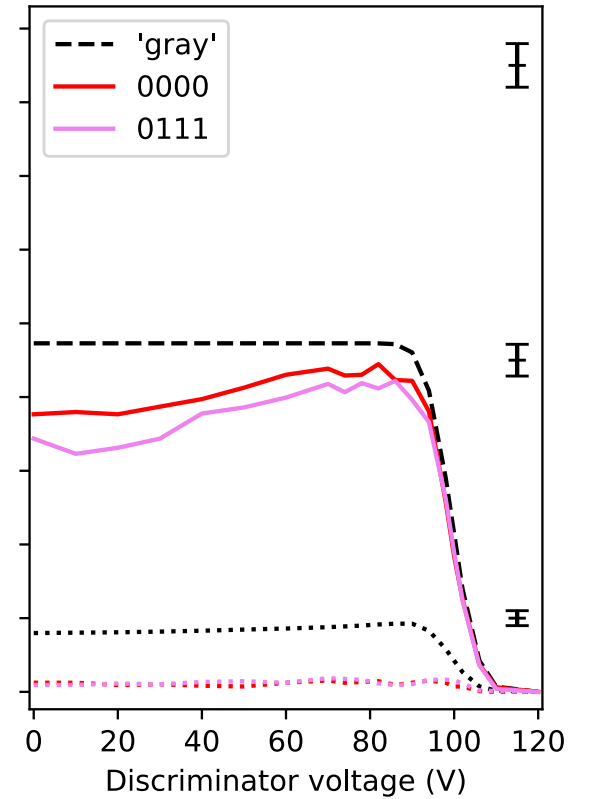
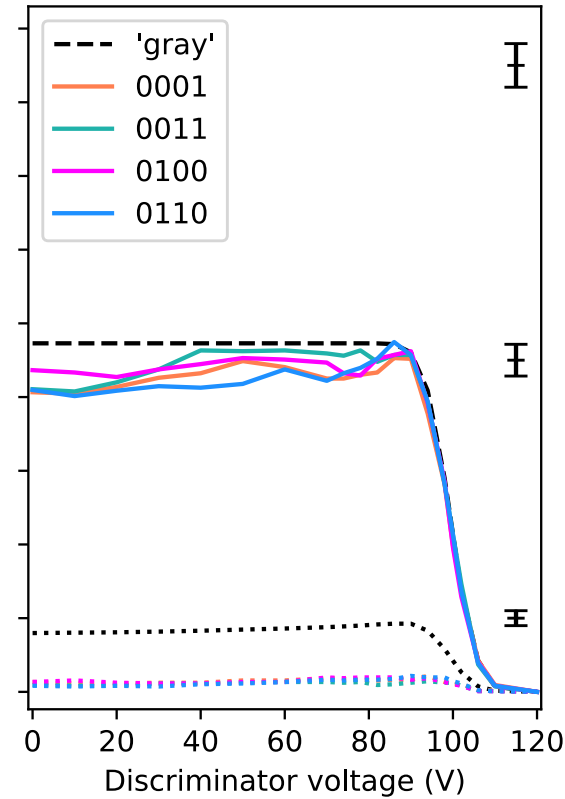
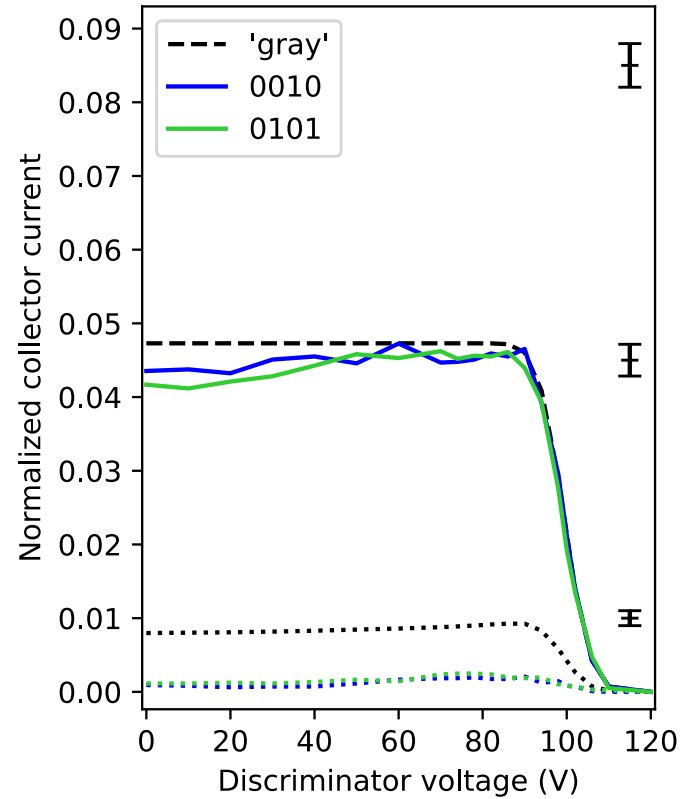
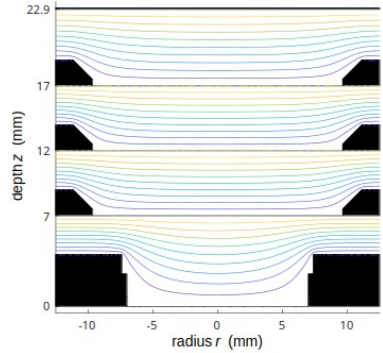
Modeling of the Retarding Potential Analyzer

Trajectories according to different models



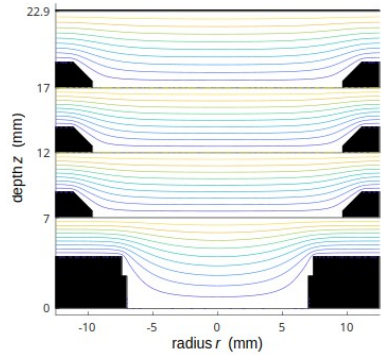
Trottenberg et al., AIP Advances 15, 035030 (2025)

Modeling of the Retarding Potential Analyzer

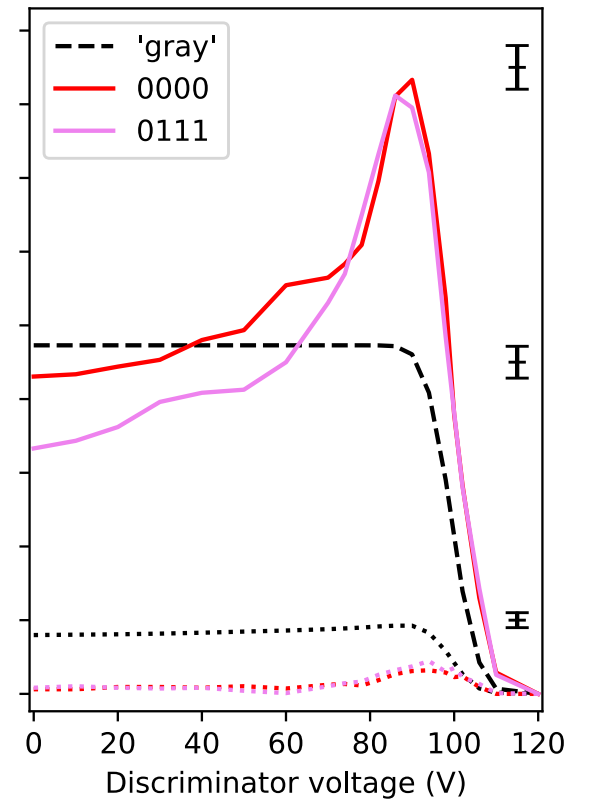
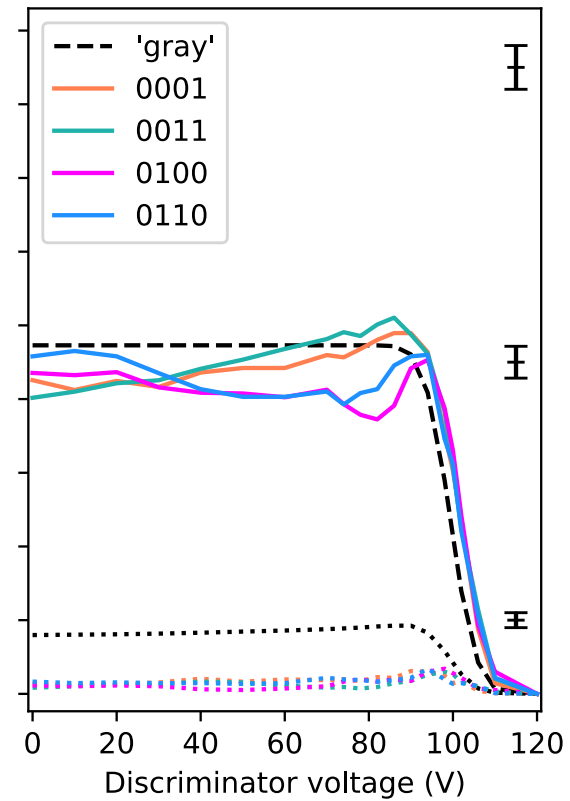
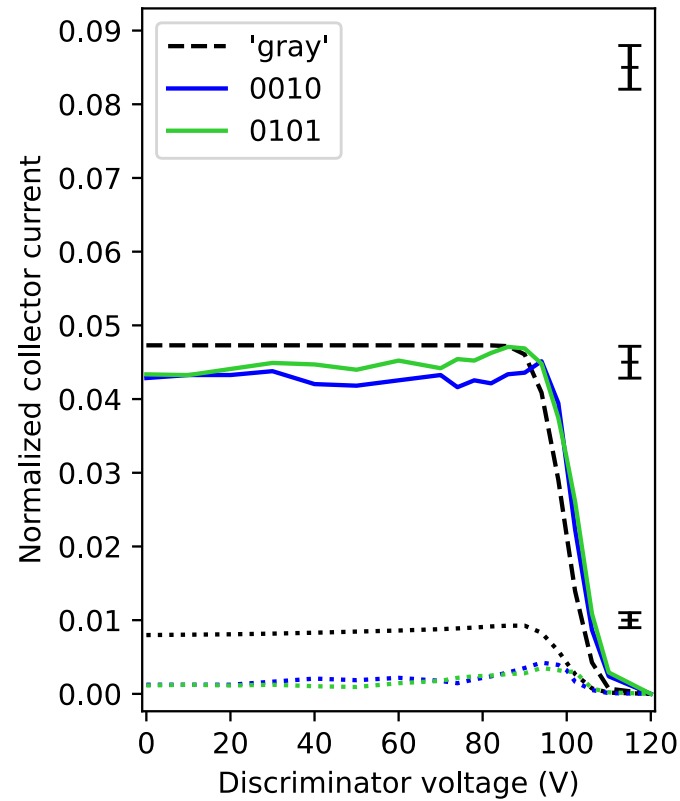
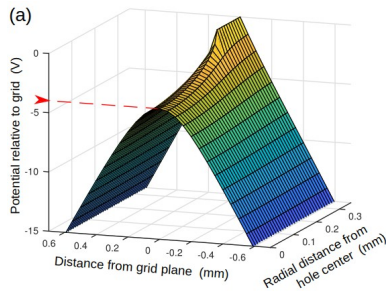


Only radial field distortion, not near fields of the holes

Modeling of the Retarding Potential Analyzer

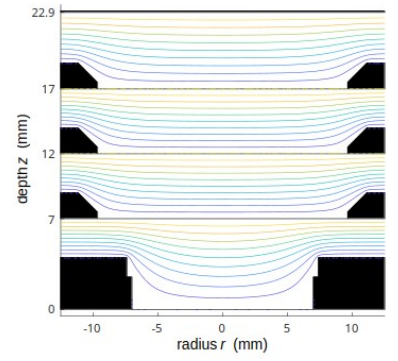


&

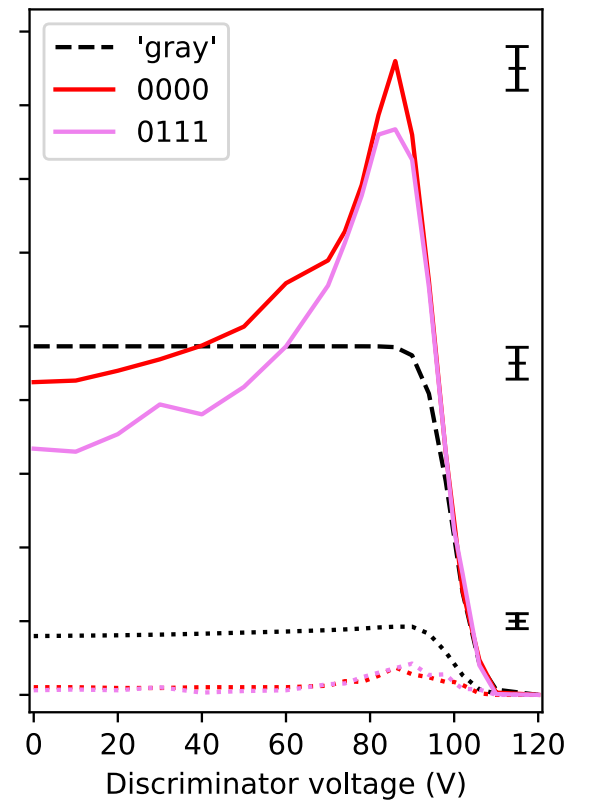
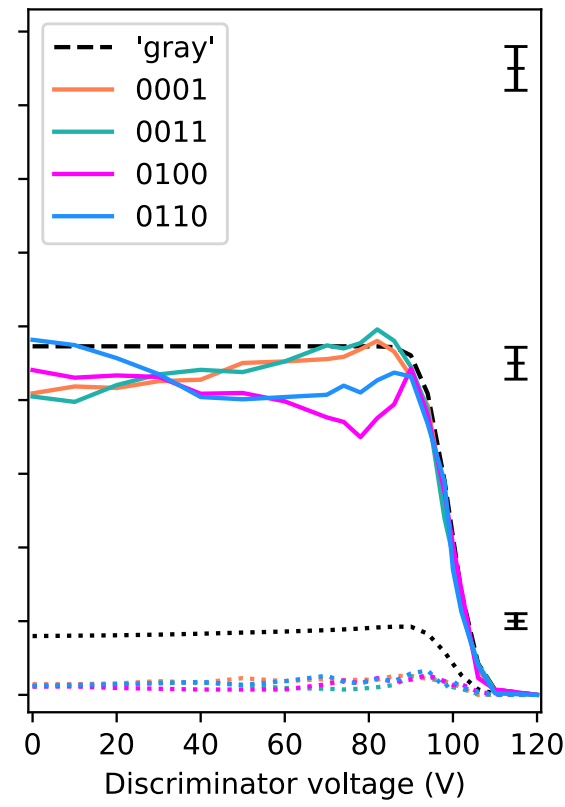
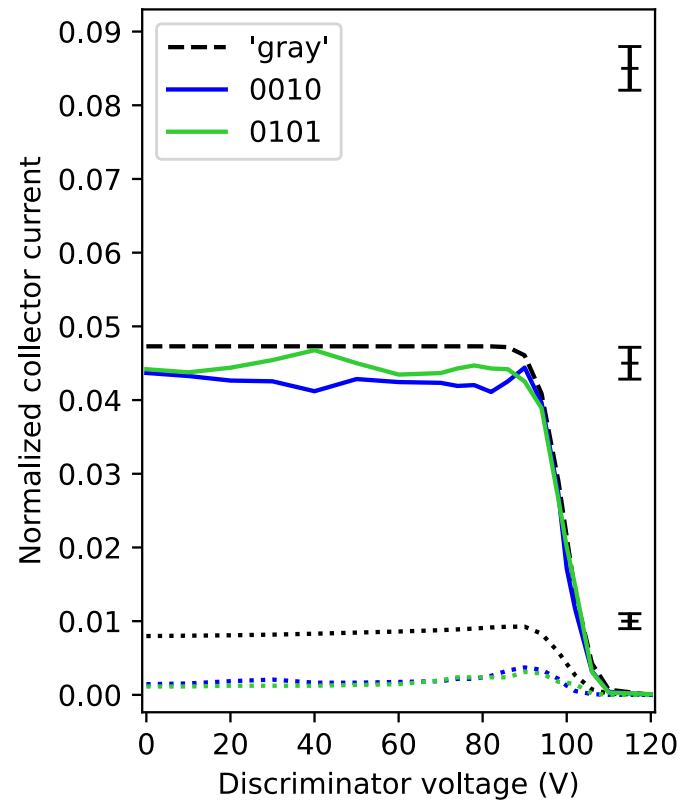
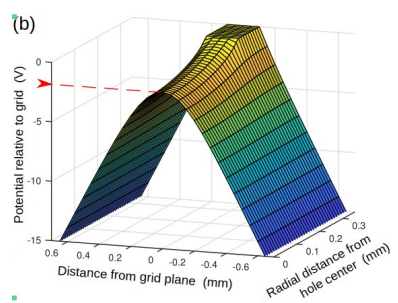


With not near fields of the holes & thin grids

Modeling of the Retarding Potential Analyzer



&



With near fields of the holes & thick grids (2 μm)

Modeling of the Retarding Potential Analyzer

With regard to the configurations, it can be stated that:

"good": Grids **3 and 4** are **not aligned**, Grid 2 is not relevant.

"intermediate": Grids **3 and 4 are aligned**, Grid 2 is aligned differently.

"bad": Grids **2, 3, and 4 are aligned**.

- The hole radius should be small compared to the grid spacing.
- The correlations of the hole positions in neighboring grids should be small,
- Irregular hole patterns could be beneficial.

Summary

Summary

- Standard diagnostics in EP
- Force probes – a useful charge-independent tool for spatially resolved momentum flux measurements
- Force probes – a tool for investigations of sputtering and validation of simulation codes
- In-flight diagnostics
- Retarding potential analyzer: The role of grid geometry and grid orientations

Acknowledgements

The development of the force probes was financially supported by the German Aerospace Center (DLR), Project No. 50 RS 1301.

The development of the EPDP was financially supported by the European Space Agency (ESA) under GSTP Contract No. 4000126205/19/NL/RA and the German Aerospace Center (DLR), Project No. 50 RS 2003.

The EPDP electronics and the erosion sensor flight models were funded by ESA, the plasma sensor was funded by DLR.

The mission specific applications of the EPDP were investigated under funding of the EPIC project within the Horizon 2020 framework programme of the European Union.